1965-06

A high-power one-millisecond pulse-forming network

Walker, William George

A HIGH-POWER ONE-MILLISECOND PULSE-FORMING NETWORK

by

WILLIAM GEORGE WALKER


.35
ACCOPRESS
GENUINE PRESSBOARD BINDER
CAT. NO. BF 2507 EMB
ACCO
CHICAGO.
LONDON.
OGDENSBURG, N.Y.
TORONTO.
MEXICO, D. F.

A HIGH-POWER ONE-MILLISECOND PULSE-FORMING NETWORK

by

WILLIAM GEORGE WALKER

S.B., United States Coast Guard Academy
(1959)

SUBMITTED IN PARTIAL FULFILLMENT OF THE
REQUIREMENTS FOR THE DEGREE OF
MASTER OF SCIENCE

at the

MASSACHUSETTS INSTITUTE OF TECHNOLOGY
June, 1965

A HIGH-POWER ONE-MILLISECOND PULSE-FORMING NETWORK

by

William George Walker

Submitted to the Department of Electrical Engineering on May 21, 1965 in partial fulfillment of the requirements for the degree of Master of Science.

ABSTRACT

Design and construction of a breadboard model of a pulse-forming network to be used in a line-type generator for a space vehicle radar system is described. The PFN is unique in that it produces a one-millisecond, high-power pulse and uses linear, ferrite-core inductors. It is designed to be space-flight worthy, reliable, efficient, and most important, the smallest and lightest weight unit that is compatible with the other pulse-generator components. A study of a pulse generator is made to determine the parameters that describe the optimum PFN. A pulse transformer and a charging reactor are discussed in detail and a description is given of the operation of the pulse generator using silicon-controlled rectifiers as switching elements.

Thesis Supervisor: J. Francis Reintjes
Title: Professor of Electrical Engineering

ACKNOWLEDGEMENT

I wish to thank James R. Sandison and Joseph A. Bosco for suggestion of this topic as a thesis subject and for the encouragement and assistance freely given and gratefully received.

TABLE OF CONTENTS

LIST OF FIGURES

LIST OF FIGURES (Continued)

CHAPTER I

INTRODUCTION

Microwave radar has resulted in the need for pulse generators capable of producing a rapid series of pulses. The convention is to use essentially rectangular pulses of high power and short duration. The length of the pulses are from a few nanoseconds to several microseconds, or more depending on the specific application.[1*] However, there have been some long duration pulse generators developed primarily for use in radio astronomy and space communication radar systems. An example of this application is the Haystack microwave research facility of M.I.T. Lincoln Laboratory.[2] A pulse generator that will produce a series of long duration (one millisecond) pulses for use in a specific space vehicle radar system presents some unique problems. Rigid restrictions on size and weight require new construction techniques to minimize these quantities.

The Electronic Systems Laboratory (ESL) at M.I.T. has a breadboard model of a space vehicle radar system for making measurements of the reflectivity of the surface of Venus. Should the experiment be formally scheduled, the vehicle would be shot at Venus on a near-miss trajectory. As it flies by, successive small portions of the surface of Venus will be illuminated with bursts of rf energy at X-band. Comparison of the reflected to transmitted energy will give a measure of surface reflectivity.[3] Signal-to-noise calculations were made at ESL based on the closest point of approach of 20,000 kilometers plus elognation of the returned echo due to curvature of the surface of Venus and relative velocity between the planet and spacecraft. These calculations resulted in peak-power and pulse-duration

---

* Superscripts refer to numbered items in the Bibliography.

transmission requirements of one kilowatt and one millisecond, respectively.[4]

This radar system uses a klystron which requires an input pulse of 8-kv at 0.60 ampere for one millisecond to produce a one kw output pulse, or a pulse generator output of

$$P_{pulse} = E_o I_o = (8,000)(0.60) = 4.8 \text{ kw per pulse} \quad (1)$$

The pulse train that this radar system will transmit in normal operation is shown in Fig. 1. Four one-millisecond pulses will be directed at each portion of the surface. A twenty-millisecond delay between pulses is required to prevent overlap of the echoes which may be elongated. A fifteen-second period between bursts is required to insure reception of the entire burst echo and change the antenna position prior to transmission of the next burst. By reference to Fig. 1, the average pulse generator output power is seen to be

$$P_{average} = \frac{\text{(total power output)}}{\text{(total period)}} = \frac{(4 \times 10^{-3})(4,800)}{15.0}$$

$$= 1.28 \text{ watts} \quad (2)$$

When considering a line-type pulse generator for use in this application, the pulse-forming network (PFN) is the most critical item since it is the bulkiest and heaviest. Analytical procedures for the design of pulse-forming networks are well established, but the physical realization of these networks for high-power application usually results in units of considerable size and weight.[1] Figure 2 shows the original PFN that was constructed by ESL for the breadboard model of this radar system. It is 22 inches long, has a volume of about 800 cubic inches and weighs 15 pounds.

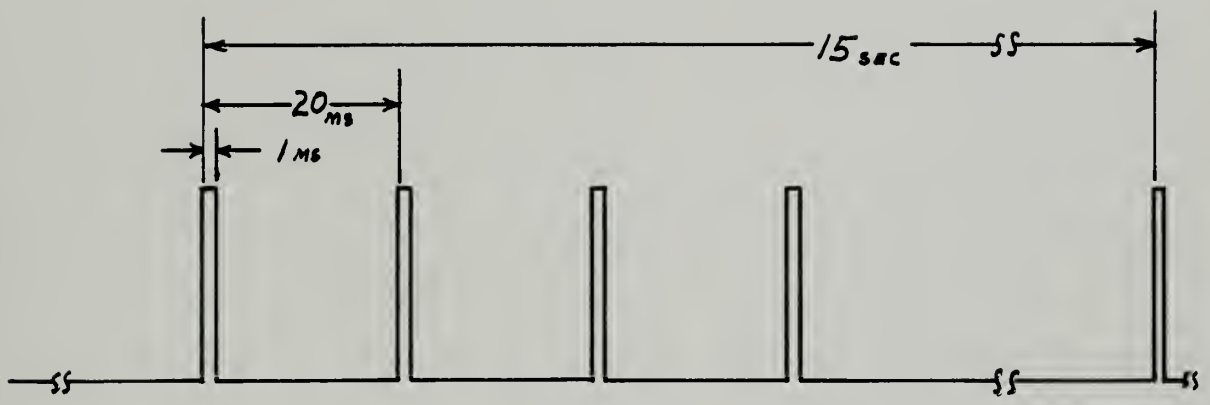

FIG. 1 RADAR TRANSMITTED PULSE TRAIN

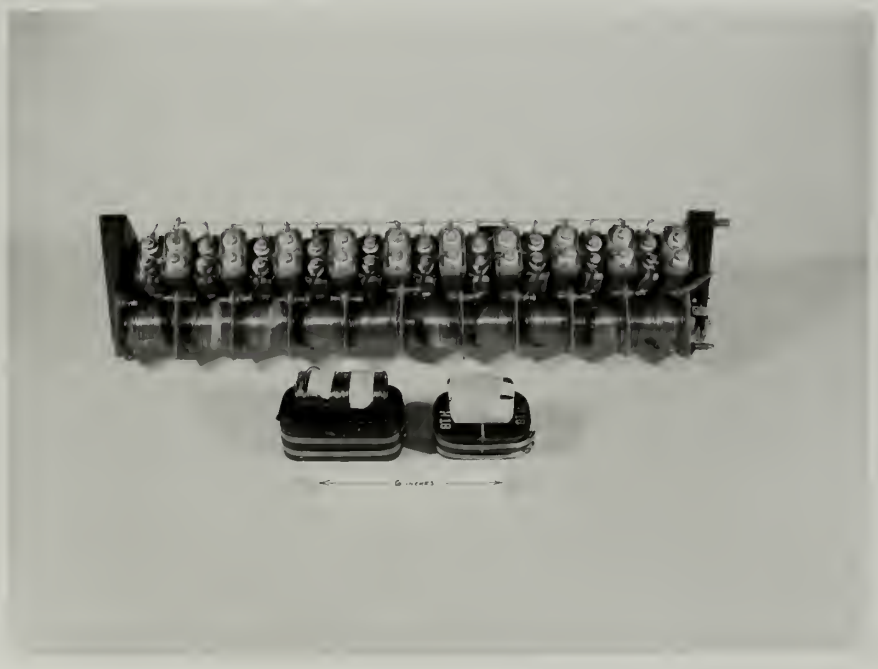

FIG. 2 ORIGINAL TEN SECTION PFN
AND CHARGING REACTOR

The reduction of size and weight was highly desired but not too easily obtained. Commerical manufacturers of pulse-forming networks declined to undertake the problem.

The object of this thesis is to design, build and test a breadboard model of an optimum PFN for a one millisecond, 4.8 kw peak power pulse generator using as criteria for optimization: 1) minimum size and weight, 2) reliability, 3) efficiency, 4) "space flight worthiness," and 5) compatibility with the other components of the pulse generator.

A PFN can be regarded as "optimum" only if its use results in the smallest and lightest weight pulse generator of this type that can be built. In order to determine the parameters that describe the optimum PFN, a study was conducted of a hypothetical pulse generator, the details of which may be found in Appendix A.

The circuit in which the PFN is used is shown in Fig. 3. This configuration meets the desire to reverse saturate, or "reset," the pulse transformer between pulses. This resetting feature reduces the chance that the pulse transformer will saturate during the long pulse. Operation of pulse generators of this and other types is described in detail in Reference 5. The pulse generator described here differs from conventional types in the use of high voltage silicon-controlled rectifiers (SCR) as switching devices.

Operation begins with the PFN initially uncharged. The power supply is assumed to have a constant d-c output of E_s volts. If losses in the system are small, the PFN will charge d-c resonantly to approximately $2E_s$ upon receipt of a timing signal at the gate electrode of SCR-1. Charging current passes to ground through the pulse transformer causing it to reset. The resetting is accomplished by a voltage appearing across the resistance R_k during the charging period. The value of R_k is set to supply just the

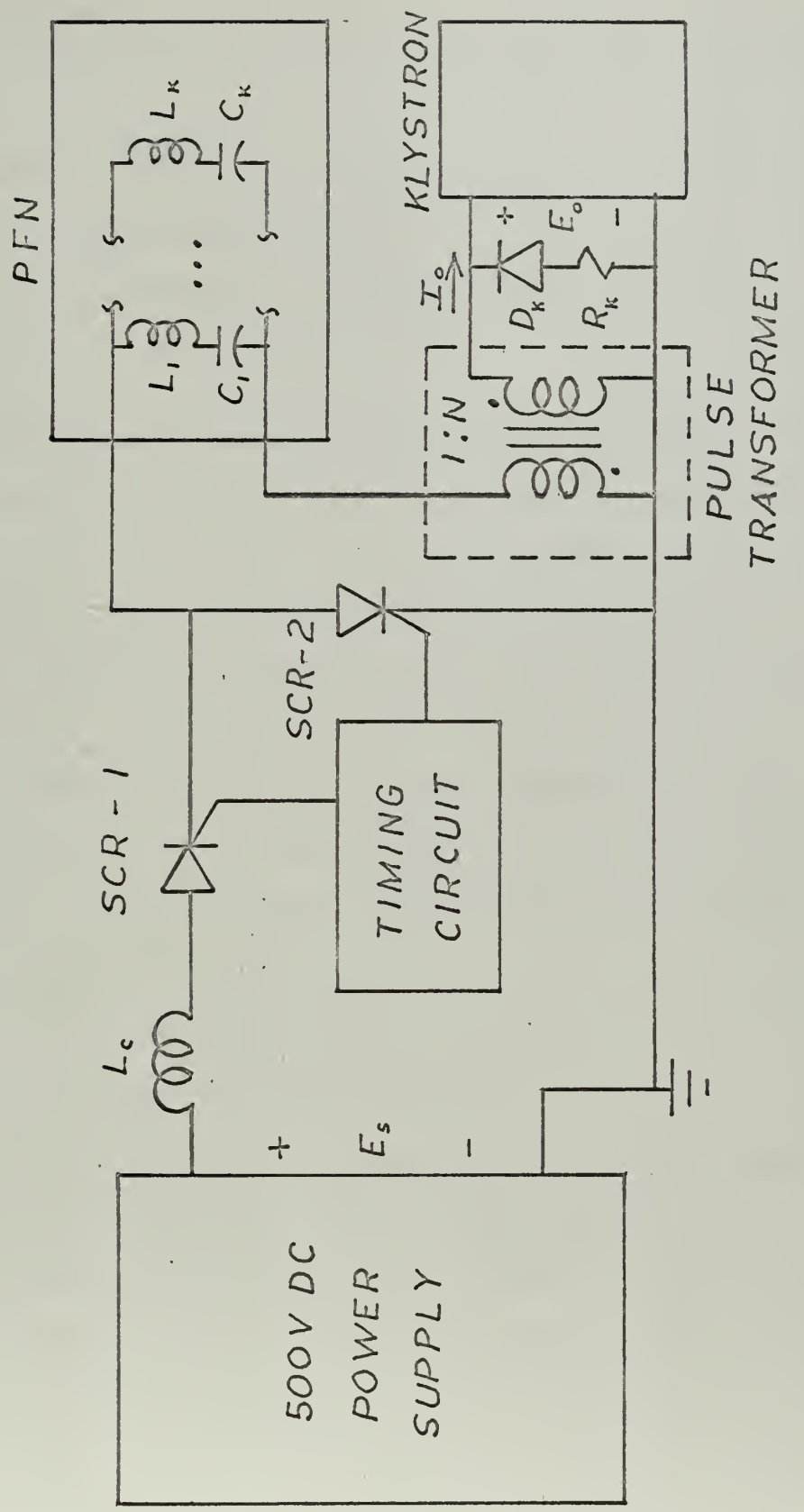

FIG. 3 BLOCK DIAGRAM OF PULSE GENERATOR

necessary voltage required to reset the pulse transformer in the interval that charging current is flowing. This charging interval is a constant value given by

$$T_c = \pi\sqrt{L_c C_n} \qquad (3)$$

where: T_c = Charging interval

L_c = Inductance of charging reactor

C_n = Total capacitance of PFN

Equation 3 is based upon the assumption that L_c is much larger than L_n, the total PFN inductance. This establishes a practical lower limit on L_c of 10 L_n. A more detailed explanation of the charging process is given in Appendix A when design of the charging reactor is discussed.

The PFN will discharge upon receipt of a timing signal at the gate electrode of SCR-2. If the impedance of the load and the characteristic impedance of the PFN are matched, the voltage appearing across the primary of the pulse transformer is an approximately rectangular pulse of amplitude E_s and duration T. The pulse transformer secondary then sees N E_s where:

T = output pulse duration

N = pulse transformer turns ratio

E_s = DC power supply output level

At the end of the pulse there will be a small amount of residual magnetizing current flowing in the primary winding of the pulse transformer. This will cause a large negative voltage spike, called "fly-back voltage," to appear across the transformer primary. The function of the diode D_k is to protect the klystron from possible damage from the fly-back voltage and to remove R_k from the circuit during discharge of the PFN. The pulse repetition rate is set by a timing circuit to meet the requirements of the radar system.

CHAPTER II

THE PULSE-FORMING NETWORK

A. DESIGN PARAMETERS

Selection of parameters to be used in designing the PFN was based on the results of Appendix A, the significant feature of which is that pulse transformer size and weight in this application are independent of other parameters for the three values of operating power supply voltage assumed. This result allowed selection of supply voltage that would simplify the PFN construction. The PFN must be constructed to operate at twice the supply voltage; therefore, the obvious choice, in this case, is 300 volts. This is the lowest value of E_s that will be available from the power supply that will actually be used in the complete pulse generator. A summary of the important parameters is given in Table 1.

Table 1

Summary of Pulse Generator Design Parameters

E_s = power supply voltage = 300 volts
N = pulse transformer turns ratio = 26.7 turns
Z_n = PFN characteristic impedance = 18.7 ohms
C_n = total PFN capacitance = 26.7 microfarads
L_n = total PFN inductance = 9.35 millihenrys
E_o = pulse transformer secondary voltage = 8,000 volts
I_o = pulse transformer secondary current = 0.6 amp
T = output pulse duration = 1.0 millisecond
a = pulse rise time factor = 5 percent
L_c = charging reactor inductance = 130 millihenrys

The PFN design procedure is as follows:[1] If losses in the pulse generator are small and the PFN is considered to be matched to the load, the pulse transformer turns ratio is approximately

$$N = \frac{E_o}{E_s} \tag{4}$$

The characteristic impedance of the pulse-forming network required for a matched load condition is

$$Z_n = \sqrt{\frac{L_n}{C_n}} = \frac{(E_o/I_o)}{N^2} \tag{5}$$

The PFN was chosen to be a five-section, type-C, Guillemin network with parameters:

$$C_n = \frac{T}{2Z_n} \tag{6}$$

$$L_n = \frac{TZ_n}{2} \tag{7}$$

The choice of PFN configuration was based upon the Fourier analysis of a periodic waveform of the type shown in Fig. 4a. This is an odd periodic function and can be used to calculate an approximation to the desired output pulse. A rectangular pulse of current can be approximated fairly well by a pulse that has parabolic leading and falling edges and a flat top, as shown in Fig. 4b.[1] The odd periodic waveform of this shape shown in Fig. 4a can be represented by a Fourier series in the form:

$$i(t) = I_p \sum_{\nu=1}^{\infty} b_\nu \sin\left(\frac{\nu \pi t}{T}\right); \quad \nu = 1, 3, 5, \ldots \tag{8}$$

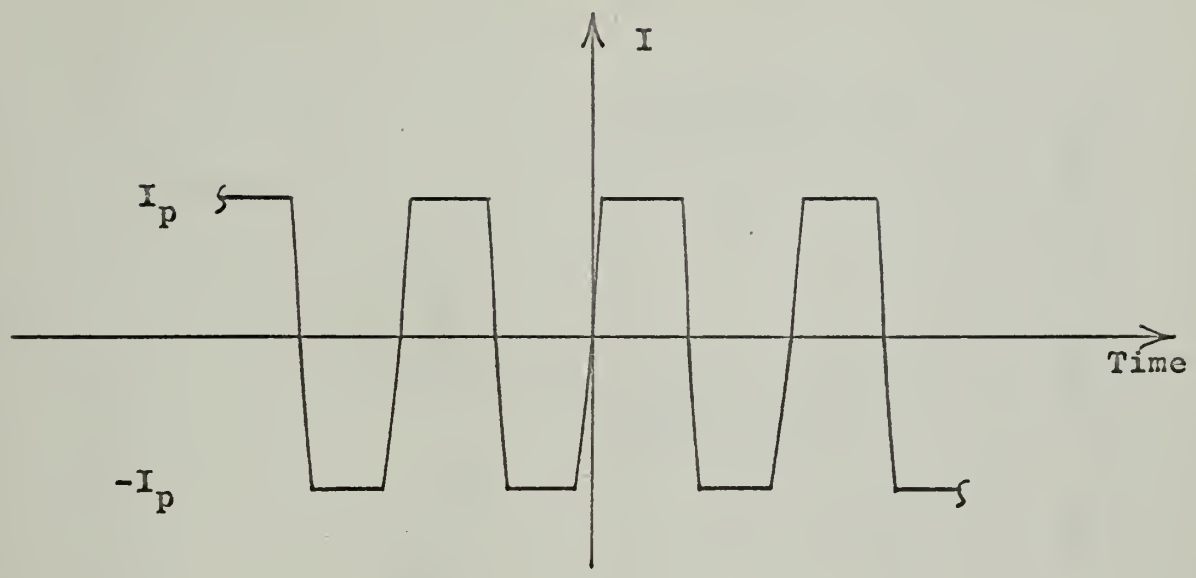

FIG. 4a. ODD PERIODIC RECTANGULAR WAVEFORM

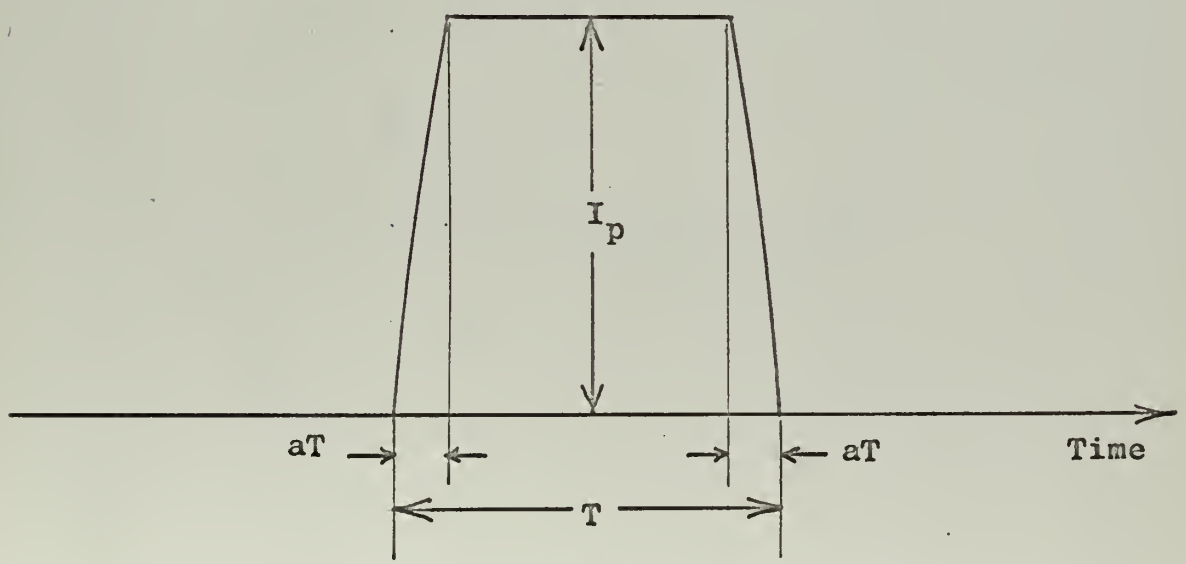

FIG. 4b. APPROXIMATION TO A RECTANGULAR PULSE

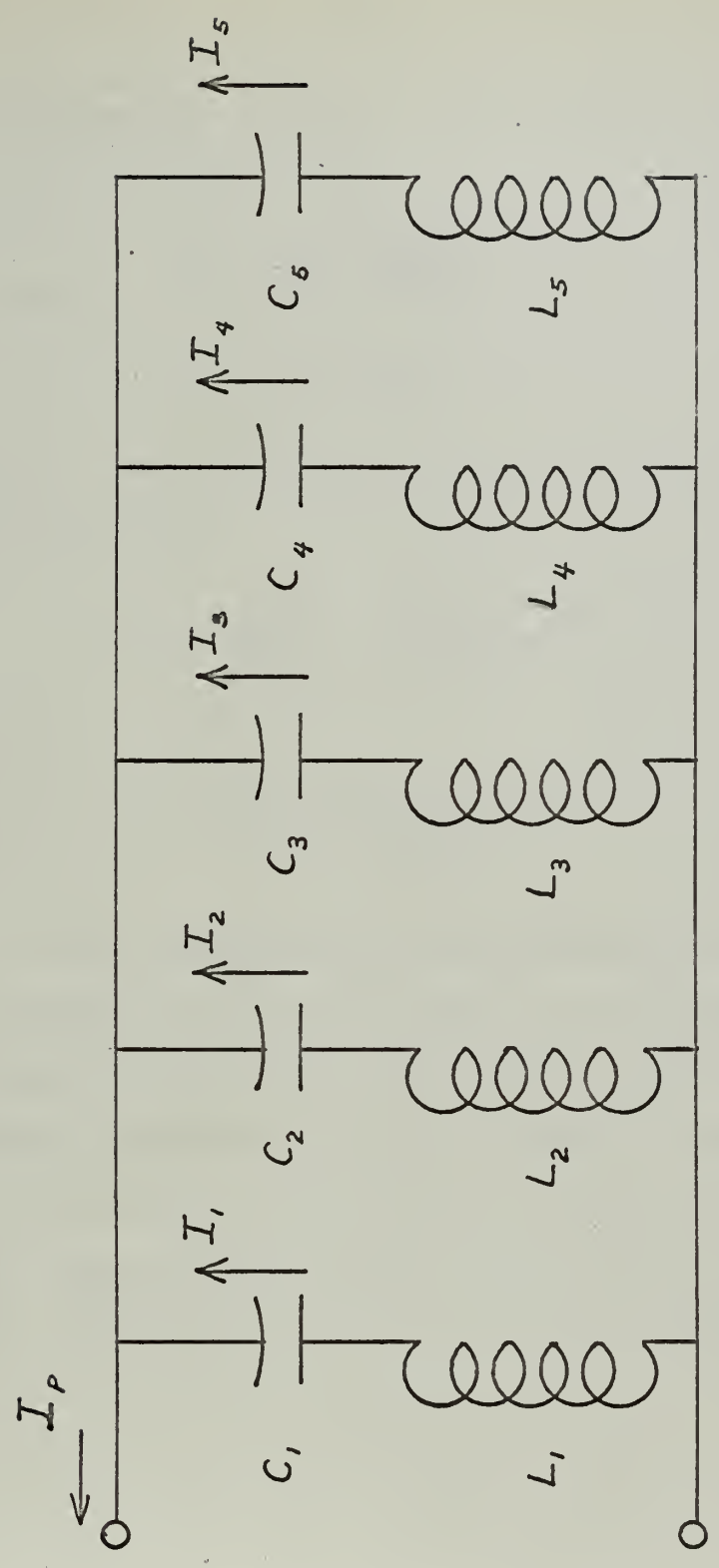

FIG. 5 FIVE SECTION TYPE-C GUILLEMIN NETWORK

Only the odd harmonics will be present, the coefficients of which are given by

$$b_\nu = \frac{4}{\nu\pi} \left(\frac{\sin \nu\pi a}{\nu\pi a}\right) \tag{9}$$

$$I_p = NI_o \tag{10}$$

A five section, type-C, Guillemin network is shown in Fig. 5. The element values are given by

$$C_k = \frac{4T}{\nu^2\pi^2 Z_n} \left(\frac{\sin \frac{1}{2}\nu\pi a}{\frac{1}{2}\nu\pi a}\right)^2 \tag{11}$$

$$L_k = \frac{Z_n T}{4} \left(\frac{\sin \frac{1}{2}\nu\pi a}{\frac{1}{2}\nu\pi a}\right)^{-2} \tag{12}$$

where: k = 1, 2, 3, 4, 5 corresponding to the appropriate network section. The calculated element values and the current $i_k(t)$ in each section of the network are given in Table 2. Examination of the values of $i_k(t)$ shows that the contribution to i(t) from the higher harmonic components decreases rapidly. The PFN was limited to five sections primarily because experience has shown[1] that addition of more sections would not improve the resulting pulse waveform significantly to warrant the additional weight and space.

Table 2

Theoretical Coefficients and Parameters
for a Five Section, Type-C, Guillemin Network

k	$C_k(\mu f)$	$L_k(mh)$	$i_k(t)$
1	21.6	4.69	$20.3 \sin (\frac{\pi t}{T})$
2	2.36	4.77	$6.65 \sin (\frac{3\pi t}{T})$
3	0.824	4.80	$3.87 \sin (\frac{5\pi t}{T})$
4	0.399	4.82	$2.67 \sin (\frac{7\pi t}{T})$
5	0.226	4.85	$1.9 \sin (\frac{9\pi t}{T})$

B. SELECTION OF MATERIALS

1. Capacitors

The capacitors used in construction of the breadboard model are a standard commerically available, high quality, 600v paper type. Size and weight are normally a consideration, but since the exact values of capacitance needed had to be obtained by combinations of standard values, size and weight of the experimental units are not too important. It is expected that single, light-weight units will be manufactured to meet space application specifications and used in place of the experimental units.

2. Inductors

a. Description of requirements. The selection of a core material was based upon a high saturation flux density. The most readily available material of this type is a grain-oriented 3% silicon steel that comes in tape-wound cores under the trade names of "Silectron,"[7] and "Hypersil."[8] Table 2 shows that the highest frequency harmonic in i(t) that will be

significant is the component 1.9 sin (ωt), where $\omega = \frac{9\pi}{T}$. This corresponds to a frequency of 4,500 cps. At this frequency the H and Z type, 4-mil cores will have reasonably small eddy current losses[7] and will be suitable for this application.

The Z-type material is preferred over the H-type because it has a slightly higher saturation flux density[8] which may allow satisfactory operation with fewer turns of wire than if the H-type were used. Otherwise either material is completely equivalent and the final choice is based upon availability.

The characteristics of Z-type Hypersil are given approximately by the B-H curve in Fig. 7. This curve shows that the permeability of the core remains essentially constant throughout most of the range of flux density and changes radically only at the extremes where saturation occurs. Pulse shape depends upon maintaining a constant value of inductance throughout the pulse period. Therefore, it is essential that operating points near saturation flux densities be avoided. The range of flux density (ΔB) was taken as 1.45 webers per square meter which is just short of the point where saturation begins as shown in Fig. 7. If the flux density is assumed to be constant over the core cross section, then the change in flux density is given by the general relationship

$$\Delta B = \frac{1}{NA} \int_0^{\tau} e(t)\, dt \qquad (13)$$

where:

A = core cross-section area
N = number of turns in coil
e(t) = applied voltage
τ = time duration of applied voltage

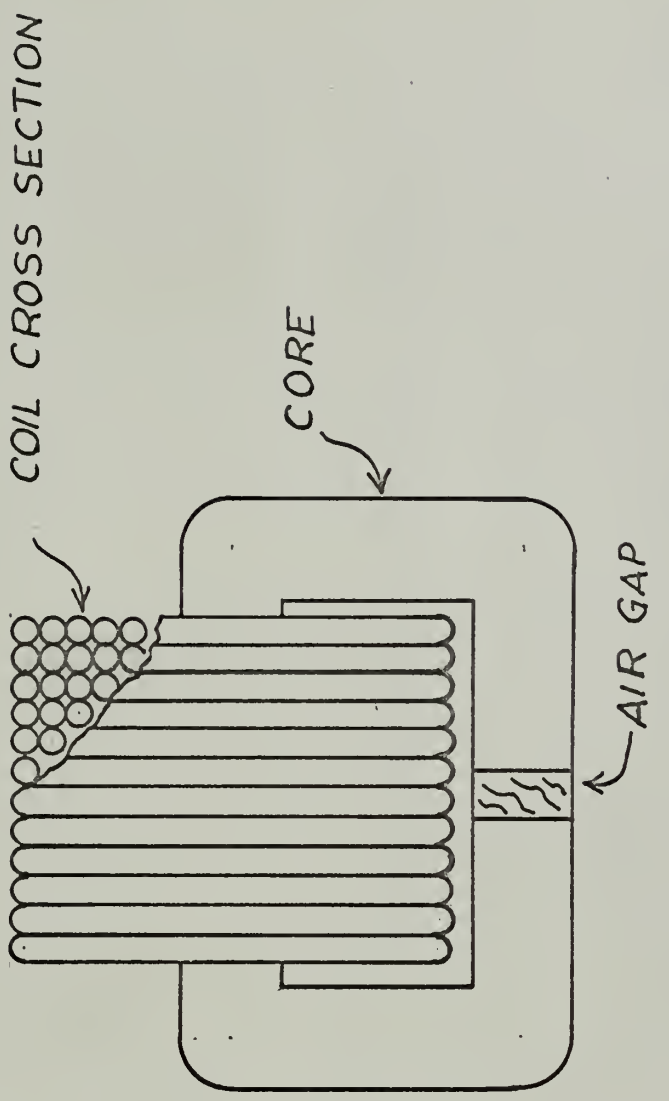

FIG. 6 INDUCTOR CONSTRUCTION

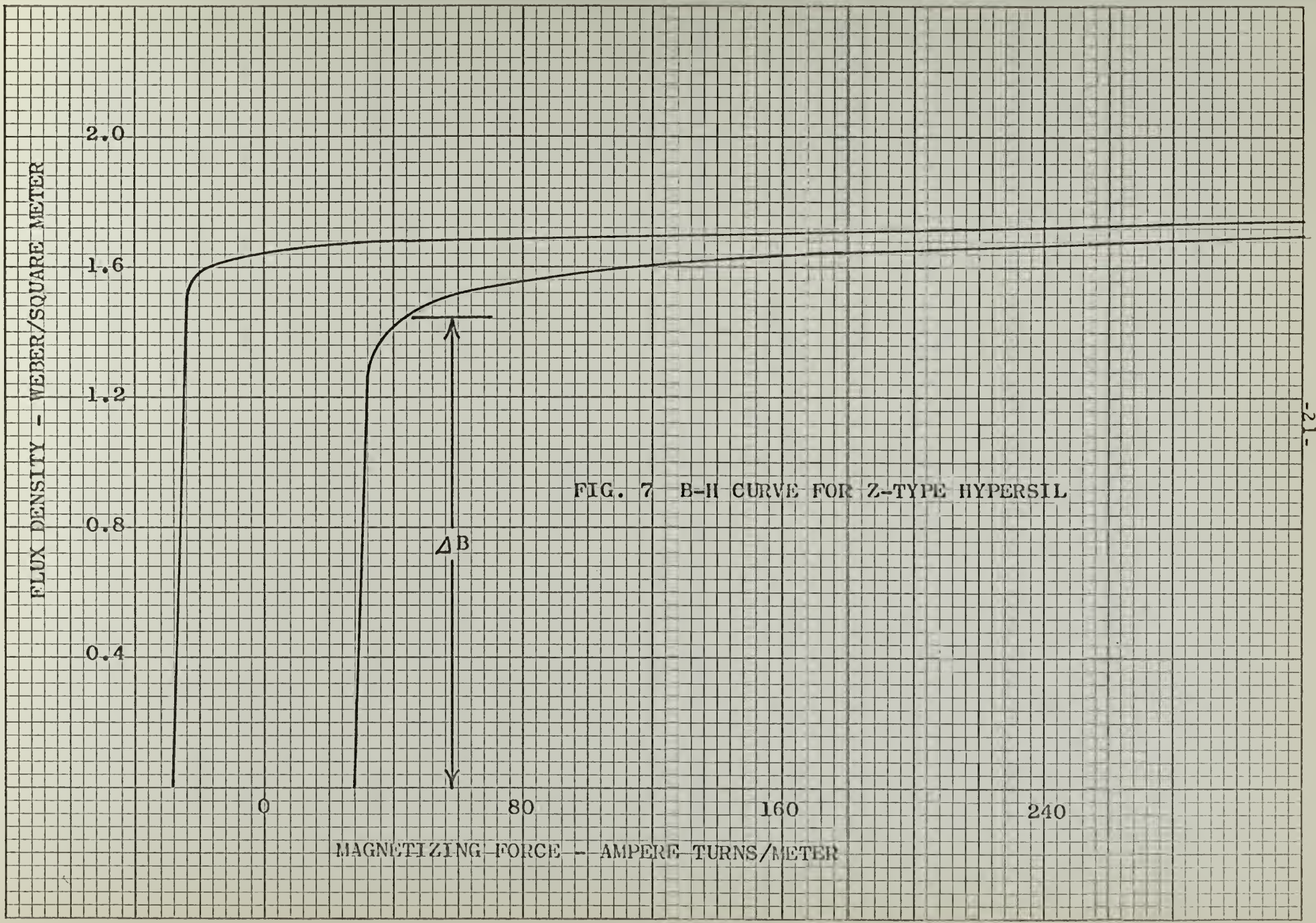

FIG. 7 B-H CURVE FOR Z-TYPE HYPERSIL

Assuming constant inductance,

$$\int_0^{\tau} e(t)\, dt = L[i(\tau) - i(0)] \qquad (14)$$

Substituting Eqs. 8 and 14 into 13 and solving for NA for the k-th inductor,

$$NA = \frac{L_k}{\Delta B} I_p\, b_\nu \sin \frac{\nu \pi \tau}{T} \qquad (15)$$

where in this case:

$$\nu = k+n \text{ for } \begin{cases} k = 1, 2, 3, \ldots \\ n = 0, 1, 2, \ldots \end{cases}$$

The cores must not saturate during the time the applied voltage is positive, or for one-half the pulse interval. Therefore, for this particular case, $\tau = T/2$ and Eq. 15 reduces to

$$NA = \frac{L_k I_p b_\nu}{\Delta B} \qquad (16)$$

At this point, all the quantities on the right of Eq. 16 are known and NA is adequately specified. It has been shown that minimizing core volume will essentially minimize losses in the inductor.[6] There are additional relationships that can be written, but there is a danger of over-specifying the core resulting in conflicting requirements and confusion. The procedure of core and wire size selection is simplified if a modified cut-and-try method is used instead of attempting to constrain all the variables. The procedure described here does minimize the core volume and is straightforward and practical.

Coil resistance is usually determined by the allowable temperature rise.[1] In this application, the peak power from Eq. 1 that must be passed

by the PFN is 4.8 kw. If power dissipated in the PFN is limited to less than five percent of the peak power, then

$$P_{dissipated} = (0.05)(4,800) = 240 \text{ watts/pulse} \tag{17}$$

Most of this power would be dissipated in inductor L_1 since it is supplying most of the total energy. A reasonable figure is to allow L_1 to consume ninety percent of the total loss.

$$P_{L_1} = (0.90)(240) = 216 \text{ watts per pulse} \tag{18}$$

Average power can be calculated from

$$P_{avg} = \frac{1}{\tau} \int_0^{\tau} R\, i^2(t)\, dt \tag{19}$$

The pulse current in L_1 taken from Table 2 is

$$i_1(t) = 20.3 \sin\left(\frac{\pi t}{T}\right) \tag{20}$$

Let $\tau = T$ and substitute Eq. 20 into Eq. 19

$$P_{L_1} = \frac{R_{L_1}(20.3)^2}{T} \int_0^{T} \sin^2\left(\frac{\pi t}{T}\right) dt \tag{21}$$

Solving Eq. 21 for R_{L_1} and using Eq. 18 gives the result

$$R_{L_1} = \frac{(2)(216)}{(20.3)^2} = 1.05 \text{ ohms} \tag{22}$$

This is a good figure to use for all of the PFN inductor coils since, as will be shown, it will result in reasonable coil sizes.

A completed coil must yield the proper value of inductance given by[1]

$$L_k = \frac{N^2 A_e \mu g}{\ell_g} \tag{23}$$

Figure 8a shows the standard type-C core that will be used with air gaps adjusted to satisfy Eq. 23. The number of turns of wire on each core is large, requiring the air gap to be relatively large. It can be assumed that most of the magnetic energy will be stored in the air gap. In this case fringing cannot be neglected and the terms are defined as:

$\mu_g = \mu_o$ the permeability of air

ℓ_g = length of air gap

A_e = effective cross section of the air gap

The effective cross section is difficult to calculate, but it can be estimated by the empirical approximation

$$A_e = \left(D + \frac{\ell_g}{2}\right)\left(E + \frac{\ell_g}{2}\right) \tag{24}$$

where D and E are the dimensions shown in Fig. 8a. Use of Eq. 24 will give an answer for inductance correct only to within a factor of 2 or 3. By adjusting the length of air gap and measuring inductance with an impedance bridge, each inductor can be set to any required value.

b. Choosing the proper core and wire size. The correct wire size can be found from reference to wire tables[11] entering the table with

$$r_w = \frac{1{,}000\, R_L}{N \ell_c} \tag{25}$$

r_w = wire resistance in "ohms per 1,000 feet"
R_L = coil resistance in ohms as given by Eq. 22
ℓ_c = average length in feet of a turn of wire

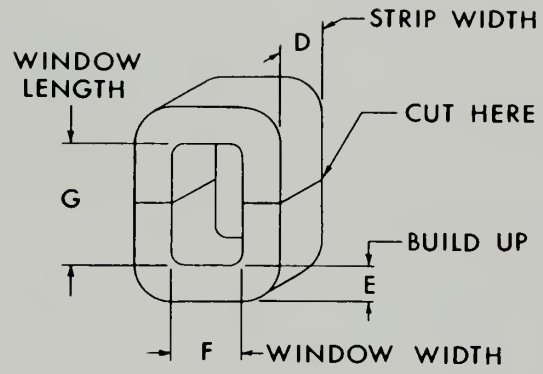

FIG. 8a. C-TYPE CUT CORE

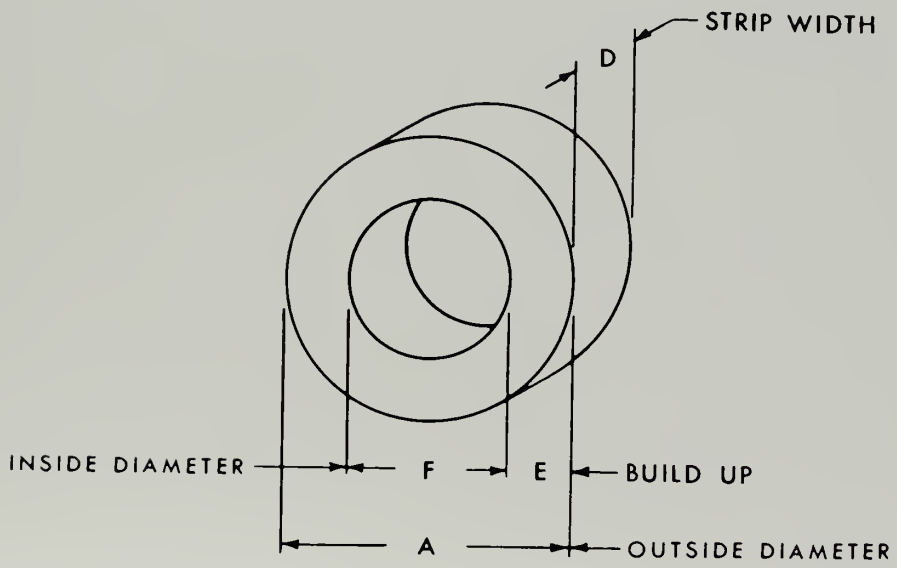

FIG. 8b. UNCUT TOROIDAL CORE

From the geometry of the core, shown in Fig. 8a, and assuming the entire window area will be used, the average length of a turn of wire is given approximately as

$$\ell_c = F + 2E + 2D \tag{26}$$

Nyclad magnet wire was used primarily because it was available in many sizes and easy to work with. The coils were hand wound on a lathe approximately as shown in Fig. 6. The required core window area for N turns of wire (size given by Eq. 25) was found with the aid of a table of turns per square inch found in Reference 11. Nyclad insulation has approximately the same insulating characteristics as Formvar which is rated at 860 volts per mil at 25°C.[12] The insulation thickness is slightly greater than one mil and there are several layers of wire on each core. The maximum operating voltage any core will be subjected to is 600 v. Therefore, the volts-per-turn is much less than the rated value and it was not necessary to insulate between layers. This provided a more compact coil and a lighter core with smaller window area was required than if an unnecessary insulating layer had been used.

The smallest core that can be used is one that has the window area, given by the product FG in Fig. 8a, completely filled with wire. For each inductor, calculations were carried out for several core sizes and the results compared in order to determine the best combination of core and coil. The choice usually came down to two cores, one had a larger cross section and was also usually heavier than the other. In each case, calculations showed the smaller core required a larger coil in order not to saturate at a given voltage level. Resistance of the two coils was the

same, about one ohm, and therefore the choice seemed easy to make--select the smaller core to minimize core losses. This did not prove to be the best choice. When these two inductors were assembled and tested, as discussed in Chapter III, the inductor with the smaller core cross section invariably saturated at a lower voltage level than was indicated by the calculations. Whereas, the inductor with a larger core cross section saturated at about the calculated level. A simple explanation for this is that the larger number of turns of wire required by the core with the smaller cross section resulted in weak linkage of flux with the core from the turns in the outermost layers. For this reason, a criteria for choosing between two theoretically equivalent cores for a given inductor is to select the core with the larger cross section.

The cores and wire sizes that were selected for the PFN inductor and the charging reactor are summarized in Table 3. The figures in this table are the result of calculations similar to the sample calculations shown in Part C of this chapter.

Table 3

List of Inductor Construction Material Characteristics

Inductor	L_1	L_2	L_3	L_4	L_5	L_6
Core number[7,8]	Z-216	H-41	Z-1	Z-4	Z-2	Z-5
Dimension (in.)						
D	0.750	0.625	0.500	0.375	0.375	0.750
E	0.375	0.250	0.250	0.187	0.187	0.375
F	0.500	0.500	0.500	0.375	0.250	0.625
G	1.500	1.312	1.125	1.000	0.625	1.250
Weight (lbs.)	0.354	0.170	0.122	0.056	0.038	0.334
Cross sec. (sq. in)	0.281	0.156	0.114	0.063	0.063	0.253
Window area (sq. in.)	0.750	0.656	0.562	0.375	0.156	0.780
ℓ_c (feet)	0.229	0.187	0.167	0.125	0.135	0.240
Wire size (AWG)[11]	19	22	24	24	24	22
r_w (ohms/1000 ft.)	8.051	16.14	25.67	25.67	25.67	16.14
Winding density (turns/sq. in.)	473	952	1,596	1.596	1,596	952

c. Typical inductor design procedures. The procedures and methods used in constructing the inductors are shown by a set of sample initial calculations for one inductor. Then it is shown how these figures had to be changed after the inductor had been tested. The sample calculations are shown in this part, whereas the testing of the inductor is the subject of Chapter III. The following calculations are the initial ones made to determine if the particular core and wire size are adequate for the element under consideration, in this case L_1. The final value of the element is given in Chapter III.

The first step is to select a core and tabulate its characteristics as shown in Table 3. With the core cross section area from Table 3 for the Z-216 core, the required number of turns of wire for L_1 can be calculated from Eq. 16

$$N = \frac{(4.69 \times 10^{-3})(16.0)(1.27)}{(1.81 \times 10^{-4})(1.45)} = 362 \text{ turns} \quad (27)$$

where:

L_1 = 4.69 millihenrys

I_p = 16.0 amperes

b_1 = 1.27

ΔB = 1.45 webers/square meter

$A = (0.281)(6.45 \times 10^{-4}) = 1.81 \times 10^{-4}$ square meters

The wire size can now be determined from Eq. 25 and a wire table

$$r_w = \frac{(1.05)(1,000)}{(362)(0.229)} = 12.7 \text{ ohms/1,000 feet} \quad (28)$$

This corresponds directly to number 21 wire, but number 20 wire was selected because of its lower resistivity. Number 20 wire has a winding density of 621 turns per square inch. The window area required to accommodate the coil winding is

$$\text{Window area} = \frac{362}{621} = 0.583 \text{ square inch} \qquad (29)$$

The Z-216 core has a window area of 0.750 square inch, therefore it would be adequate for this inductor.

The required air gap can be estimated with the aid of Eqs. 23 and 24. If an air gap of one inch on each side of the core is assumed, Eq. 23 becomes

$$A_e = (1.750)(1.375)(6.45 \times 10^{-4}) = 15.5 \times 10^{-4} \text{ sq. meters} \qquad (30)$$

and the inductance is approximately

$$L_1 = \frac{(362)^2(15.5 \times 10^{-4})\,(4\pi \times 10^{-7})}{(2)\,(2.54 \times 10^{-2})} = 5.03 \text{ millihenrys} \qquad (31)$$

Equation 31 shows that a total air gap of two inches will give approximately the required inductance for L_1. Exactly the required value of inductance can be obtained by shimming the air gap and measuring inductance with an impedance bridge.

This is the extent of the initial calculations that were made for each PFN inductor. Based upon these calculations the five PFN inductors were constructed and assembled for tests as shown in Fig. 11a. Figure 11b shows the completed breadboard model which is the final version of the PFN. Preliminary versions differed from this photo only in that capacitance decade boxes, which were easier to manipulate during tests, replaced the capacitors shown. The exact nature and extent of the tests performed on the PFN are described in Chapter III.

CHAPTER III

TESTING THE PULSE FORMING NETWORK

A. MEASUREMENT OF INDUCTOR CORE SATURATION VOLTAGE LEVEL

It was desirable to determine if the individual inductors would perform satisfactorily under normal operating conditions without having to assemble and test the complete PFN. Equation (13) states that the flux density in a ferrite core inductor is proportional to the time integral of the voltage applied across the coil terminals. This assumes that the resistance of the coil is zero, or at least very small compared to the coil reactance. When the coil resistance cannot be ignored, the circuit of Fig. 9 can be used to subtract the voltage drop caused by the coil resistance and display a picture of the hysteresis loop, which in this case would be more accurately described as a plot of coil flux versus coil current.[10]

The operation of this circuit is as follows: By summing the currents at point Y

$$i_c = i_{R_1} + i_{R_2} \tag{32}$$

Which is

$$C\frac{dv_c}{dt} = \frac{v_{R_1}}{R_1} + \frac{v_{R_2}}{R_2} = \frac{v - v_c}{R_1} + \frac{v_R - v_c}{R_2} \tag{33}$$

where:

$v = v_L + v_r$ = coil voltage in volts

i = inductor current in amperes

r = inductor coil resistance in ohms

R = 10 ohm, 50 watt potentiometer

C = one microfarad

$R_1 = R_2$ = one megohm

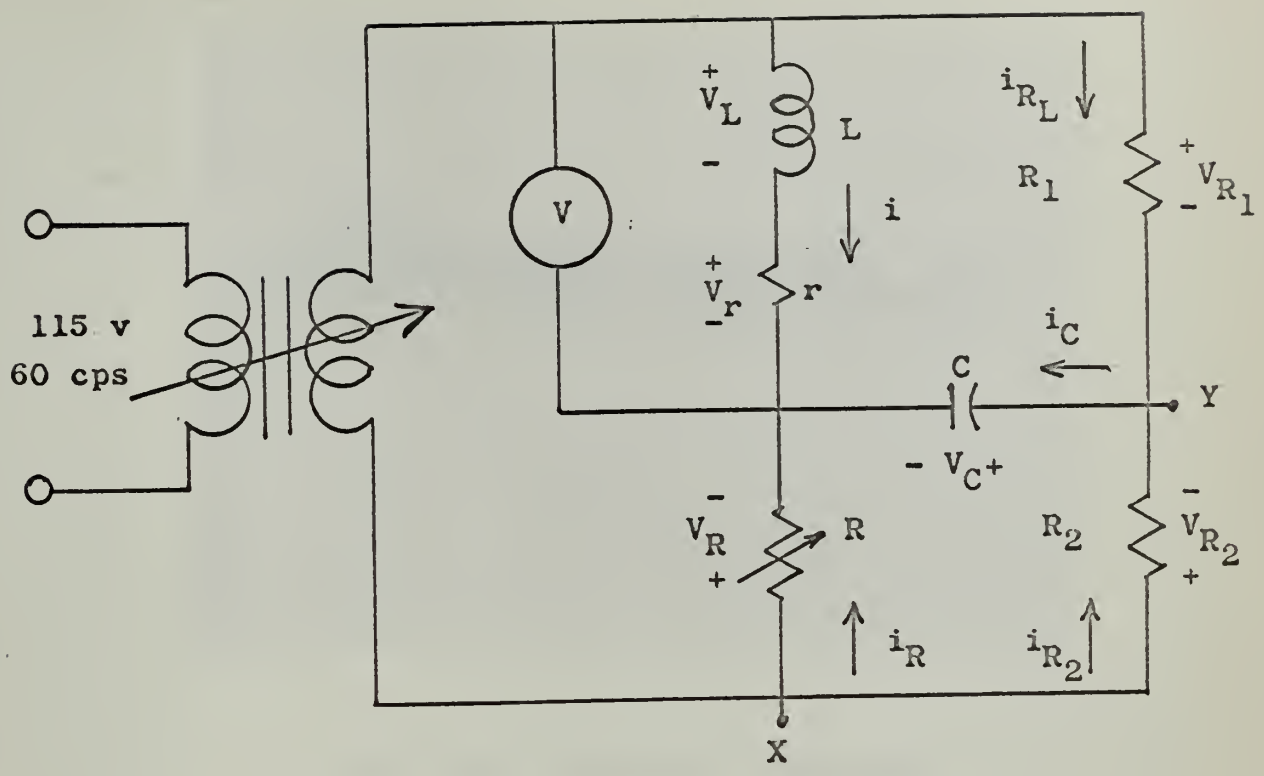

FIG. 9 CIRCUIT FOR DISPLAYING INDUCTOR CORE SATURATION VOLTAGE LEVEL

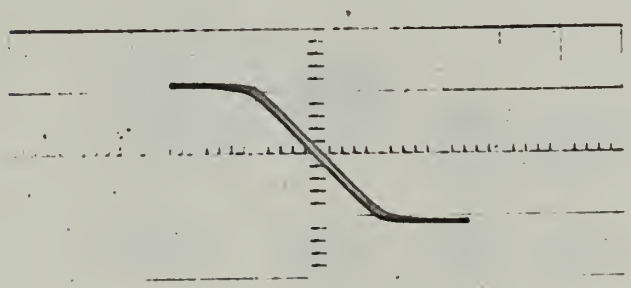

20 volts/cm

20 volts/cm

FIG. 10 CORE HYSTERESIS LOOP

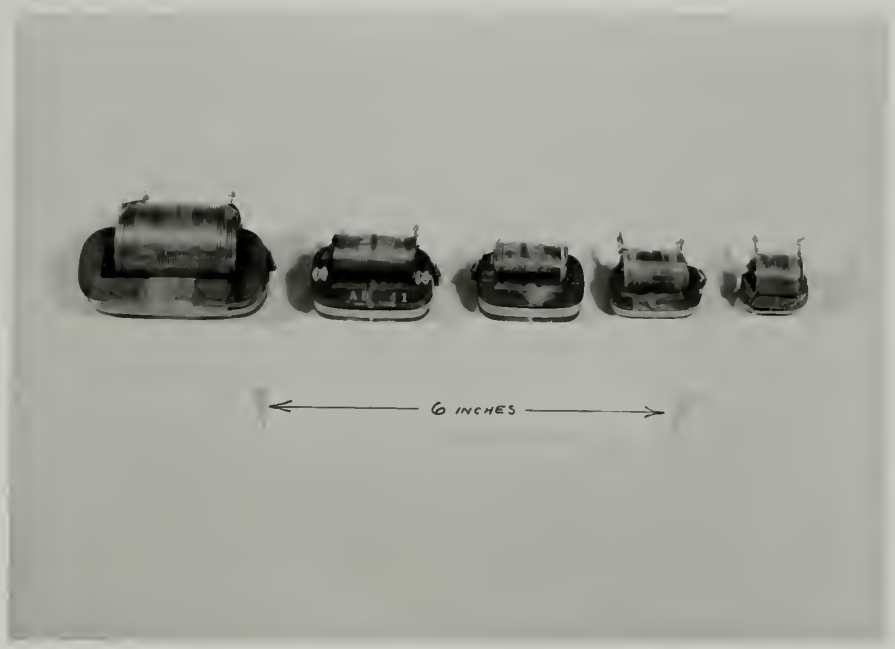

FIG. 11a FIVE PFN INDUCTORS

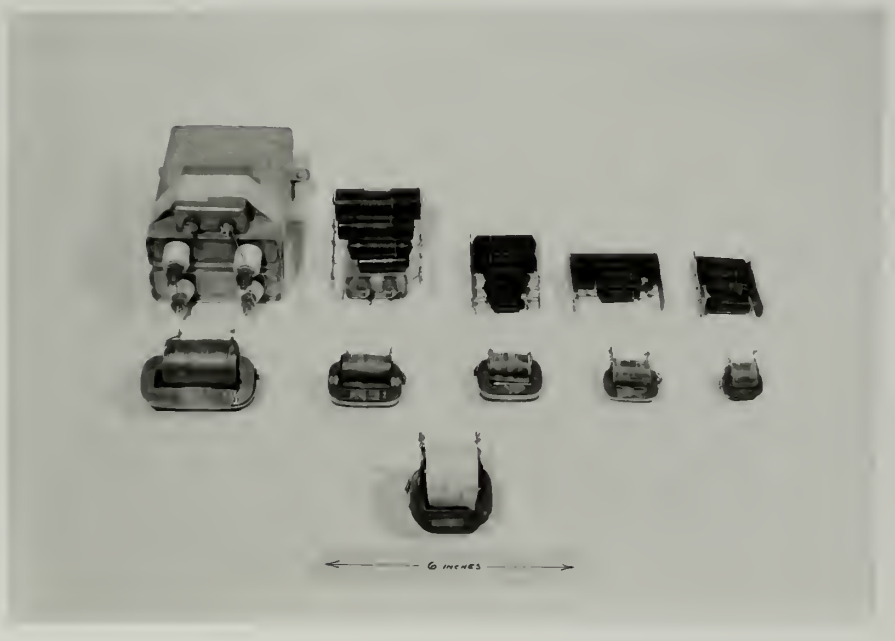

FIG. 11b BREADBOARD MODEL OF THE PFN AND THE CHARGING REACTOR

The resistance of the parallel combination of R_1 and R_2 will be much larger than the reactance of C at 60 cps. The reactance of the coil is also small and if we measure the coil resistance and set R to this value, the current in the coil, and in R will be much larger than i_{R_1} or i_{R_2}. On this basis the following approximations can be made:

$$v_R = -ir$$

$$\frac{v_c}{R_1} = \frac{v_c}{R_2} = 0 \tag{34}$$

Then equation (33) can be written

$$v_c = \frac{1}{CR_1} \int v dt - \frac{R}{CR_2} \int i dt \tag{35}$$

But

$$R_2 = \frac{R R_1}{r}$$

therefore

$$v_c = \frac{1}{CR_1} \int (v - ir)\, dt \tag{36}$$

The hysteresis loop of the inductor core can be viewed directly by connecting the horizontal and vertical amplifiers of an oscilloscope to points x and y, respectively.

This circuit is used by first calculating the flux density level that the inductor must absorb under operating conditions and relating this level to an rms voltage reading across the coil. Sample calculations are given here for L_1.

The voltage drop across an inductor coil is

$$e(t) = L\frac{di(t)}{dt} \tag{37}$$

Coil current in L_1 under operating conditions is

$$i(t) = I_o \sin \frac{\pi t}{T} \tag{38}$$

$$e(t) = L I_o \frac{\pi}{T} \cos \frac{\pi t}{T} \tag{39}$$

The flux density level is

$$B = \int_0^T e(t)\, dt = L I_o \tag{40}$$

This corresponds to one-half the total change in flux density that a PFN inductor will experience during a discharge pulse. It is required that the inductance remain constant during this interval or that the flux density remain in the linear region of the hysteresis curve

$$2 \int_0^\tau e(t)dt = (2)(4.69 \times 10^{-3})(20.3) = 0.190 \text{ volt-seconds} \tag{41}$$

at 60 cps this corresponds to a voltage across the inductor of

$$V = \frac{(0.190)(0.707)}{0.00833} = 16.1 \text{ volts RMS} \tag{42}$$

This must be the minimum voltage reading at the point where the curve of Fig. 10 begins to change slope in order to insure a constant value of inductance during a pulse.

Figure 10 shows the hysteresis loop obtained for L_1 by this method. The voltage level corresponding to the point where the core begins to saturate is 19.0 volts RMS. This result indicates that this inductor should perform satisfactorily in the PFN under normal operating conditions.

B. CONSTRUCTION OF THE PFN TESTING CIRCUIT

The PFN was tested by observing its output pulse waveform. In order to do this it was necessary to assemble the pulse generator shown in Fig. 3. For testing the network a dummy load, as shown in Fig. 12, was used in place of the pulse transformer, klystron, and elements D_k and R_k. R_L is made variable to provide an exact matched load for the PFN. The output pulse waveform referred to is the voltage appearing across R_L when PFN discharges. The function of the diode is to remove R_L from the circuit while charging the PFN to improve charging efficiency.

The power supply used was a large nonregulated d-c unit that was available in the laboratory. It was arranged with a variac to allow the output voltage to be varied from 0 to 500 volts and a current limiting circuit breaker arrangement to protect it from overloads during tests.

The charging reactor for the test circuit could have been any reactor that had low coil resistance, provided a satisfactory charging interval and did not saturate. The one that was used throughout all the tests is the reactor described in detail in Appendix A and referred to in Tables 1, 3, and 7.

The timing circuit and switching SCR's are discussed in detail in Appendix B. This part of the test circuit requires a lengthy discussion to properly emphasize its importance in the design of this type of pulse generator. However, this discussion is not pertinent to the actual testing of the PFN and is deferred to a later part.

C. CORRECTION OF THE PFN OUTPUT PULSE WAVEFORM

Requirements that the output pulse waveform must meet can be summarized as follows: 1) rise time from the 0 to 90 percent level less than 50 microseconds, 2) overshoot and ripple less than 10 percent,

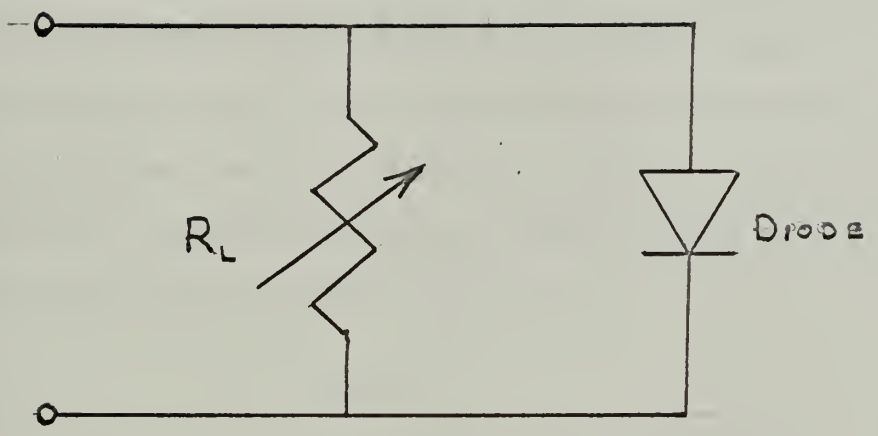

Fig. 12 Dummy Load for Testing PFN

3) approximately one millisecond in duration, 4) contain 4.8 joules of energy. Item number 4 is significant, but it was not actually measured until the final waveform was obtained and the PFN efficiency was calculated. The first three items are covered in this section.

The first version of the PFN that was tested had approximately the element values calculated from the theoretical discussion of Chapter II. The actual measured element values differed slightly from the theoretical because it was difficult to adjust the inductor air gaps precisely using plexiglas stock and mylar shims which was the method used to obtain the required air gap. The element values for the first PFN version are listed in Table 4. The resulting output pulse waveform is shown in Fig. 13. This pulse meets rise time and duration requirements, but the ripple is about 25 percent and gets worse toward the end of the pulse.

Table 4

Element Values for the First Version of the PFN

k	Measured L_k(mh)	Measured C_k(μf)
1	4.70	21.5
2	4.80	3.1
3	4.97	0.775
4	4.80	0.370
5	5.05	0.180

Reference 1 indicated that an increase of sixteen percent over the theoretical values of inductance resulted in substantially improved waveform. In order to determine the amount of increase required in this case, the following approximations were made:

$$\sqrt{L_1 C_1} = T/\pi \tag{43}$$

$$\sqrt{\frac{L_1}{C_1}} = Z_n \tag{44}$$

Z_n = 18 ohms (approximately)

T = one millisecond

Solving these equations yields

$$L_1 = 5.75 \text{ mh}$$

$$C_1 = 17.5 \ \mu\text{f} \tag{45}$$

This is an increase of twenty-three percent over the theoretical value of L_1.

The second version of the PFN was made by increasing the inductance values all by approximately twenty-three percent. These element values are listed in Table 5.

Table 5

Element Values for the Second Version of the PFN

k	Calculated L_k(mh)	Measured L_k(mh)	Measured C_k(μf)
1	5.75	5.75	15.0
2	5.85	5.85	1.512
3	5.88	6.05	0.495
4	5.90	6.00	0.241
5	5.95	6.20	0.130

The resulting output pulse waveform is shown in Fig. 14. This pulse has an undesirable overshoot of about twenty-five percent and is also too narrow. In order to reduce the overshoot, the amplitudes of the higher harmonics

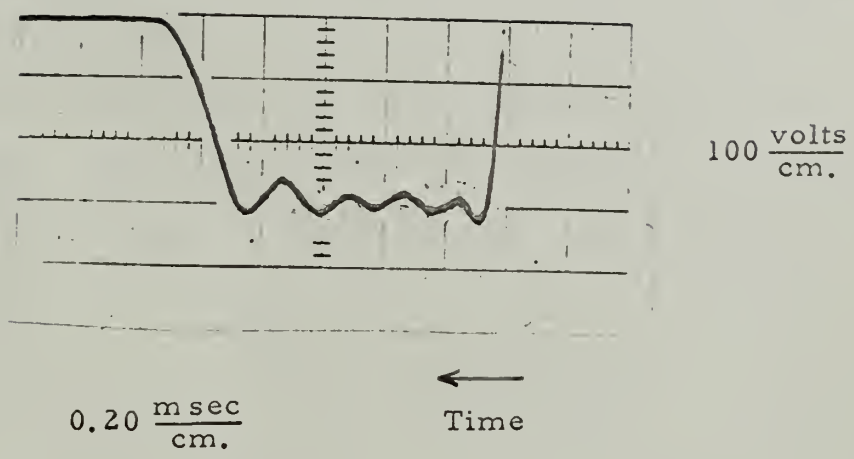

Fig. 13 Output Pulse Waveform from the First PFN Version

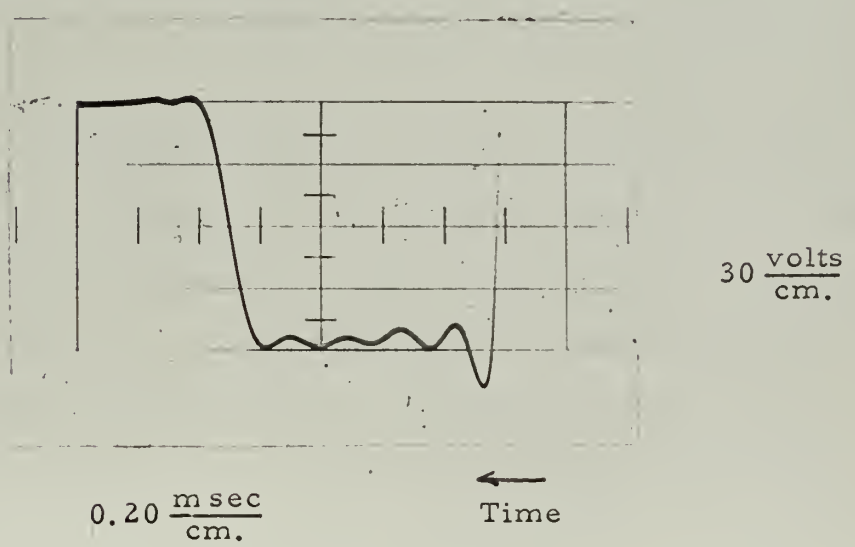

Fig. 14 Output Pulse Waveform from the Second PFN Version

were decreased by successively increasing the values of inductance.

The final version of the PFN was arrived at by trial-and-error adjustments of element values until a satisfactory pulse waveform was obtained. This waveform is shown in Fig. 15a and the element values are summarized in Table 6. This waveform meets the first three requirements verywell. Figure 15b shows the rise time to the ninty percent voltage level is less than fifty microseconds. Figure 15a shows the pulse duration is approximately one millisecond, and the overshoot and ripple are less than ten percent.

Table 6

Element Values for the Final Version of the PFN

k	L_k(mh)	C_k(μf)
1	5.80	19.7
2	6.25	1.60
3	7.40	0.464
4	8.30	0.194
5	9.35	0.103

The adjustment of inductance values for the final version of the PFN was carried out with E_s = 100 volts. When the supply voltage was increased to give a 300 volt output pulse, the pulse shape became distorted indicating core saturation was beginning. This was remedied by recalculating the number of turns required on each inductor, as shown here for L_1, and making the additions.

$$N = \frac{5.80 \times 10^{-3} \times 16.0 \times 1.27}{1.81 \times 10^{-4} \times 1.45} = 445 \text{ turns} \qquad (46)$$

$$r_w = \frac{1.0 \times 1,000}{445 \times 0.229} = 9.8 \text{ ohms/1,000 ft.} \qquad (47)$$

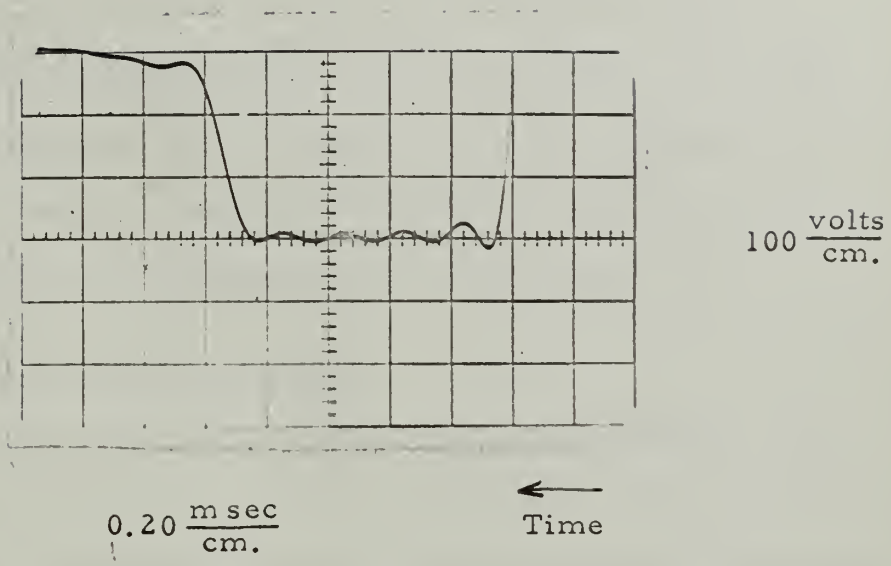

Fig. 15a Output Pulse Waveform from the Final PFN Version

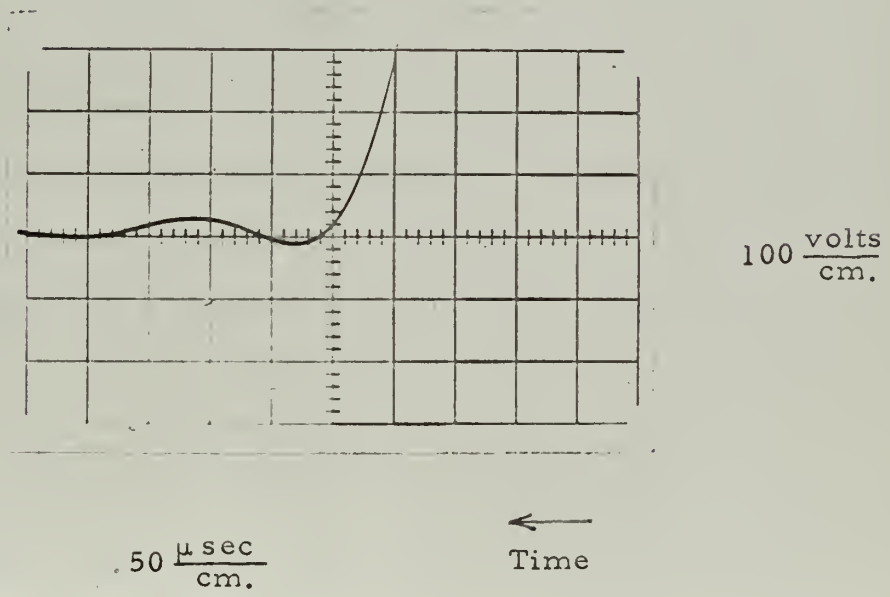

Fig. 15b Leading Edge of the Final Output Pulse Waveform

This corresponds to number 19 wire which has a winding density of 473 turns per square meter.

$$\text{Window required} = \frac{445}{473} = 0.94 \text{ square inch} \qquad (48)$$

This is larger than the window of the Z-216 core, but the additional wire was accommodated by taking advantage of the large air gap which increased the effective window area to approximately one square inch.

D. MEASUREMENT OF PFN EFFICIENCY

The efficiency of the PFN is difficult to describe independently. The effects of the charging reactor must also be included in the efficiency figure for the PFN. Figure 17 shows that for a d-c power supply level of 240 volts, the PFN charges to 450 volts in about five milliseconds. The d-c resistance of the PFN is about 0.2 ohm and the charging reactor resistance is 3.84 ohms. Substituting this value of resistance into Eq. 78 gives

$$v(T_c) = 1.925 \times E_s = 462 \text{ volts} \qquad (49)$$

The attenuation of the PFN voltage could be reduced but only by making a larger reactor coil winding to reduce coil resistance resulting in a heavier element. The resulting pulse voltage level is shown in Fig. 17 as 200 volts. When the PFN discharges, each inductor dissipates some power due to its own winding resistance of about one ohm. This loss shows up as a lower level output pulse than would be expected if the PFN were lossless.

The PFN was tested with full power at a continuous repitition rate of 20 msec between pulses. The average power input to the pulse generator from the power supply was measured as

FIG. 16

GRAPH of VOLTAGE-SQUARED vs TIME
FOR AN OUTPUT PULSE

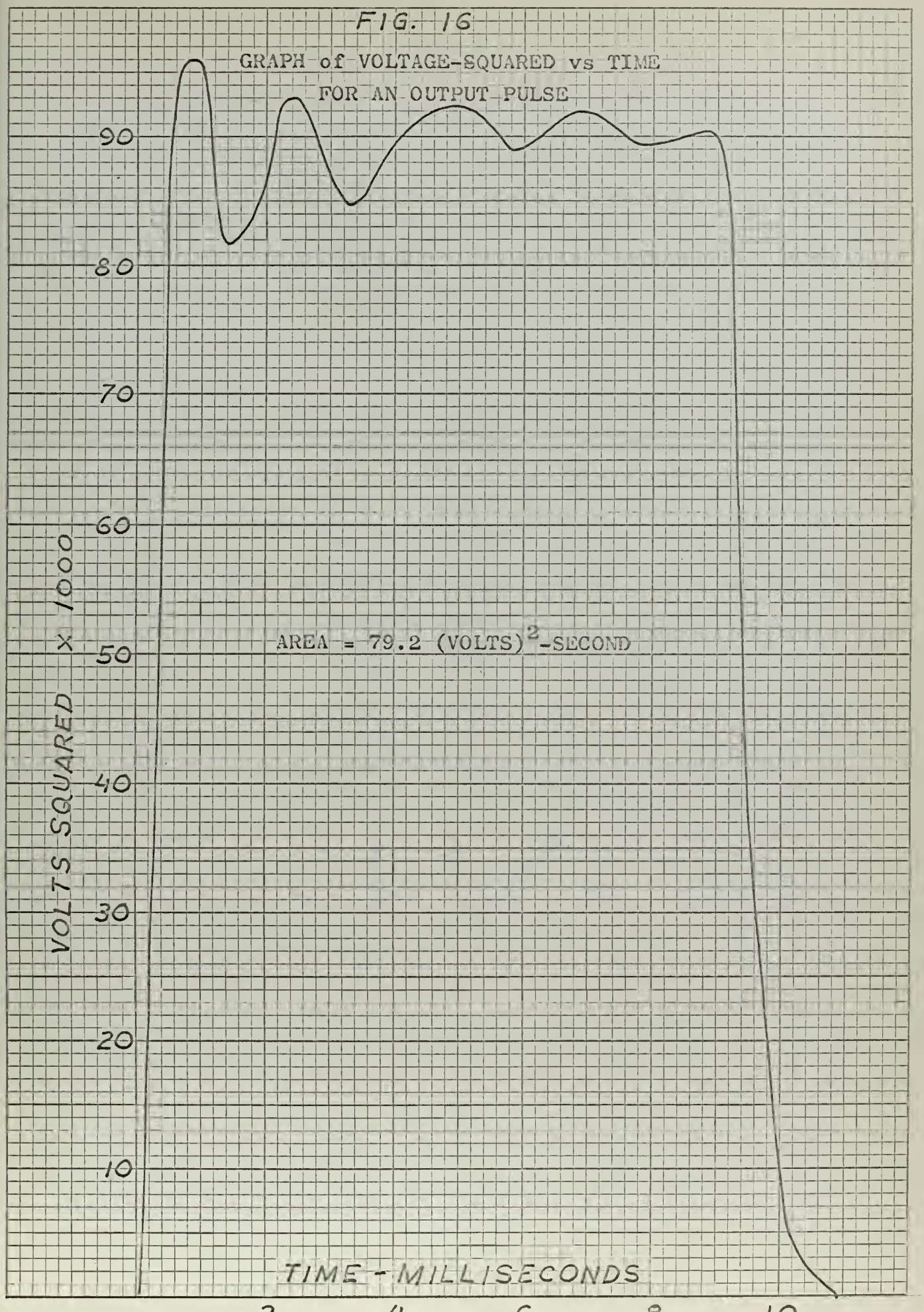

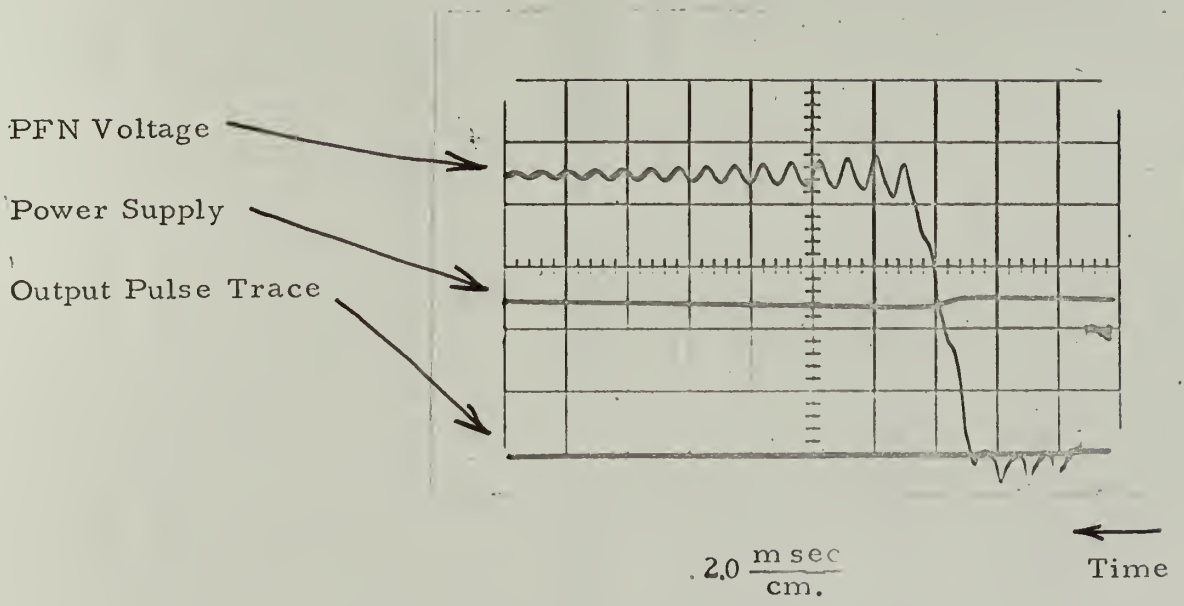

Fig. 17 Relation Between Power Supply Voltage, PFN Voltage and Output Pulse Voltage Level

$$\overline{P_{in}} = I_s E_s = 0.75 \times 380 = 285 \text{ watts} \tag{50}$$

I_s = power supply output current in amperes

E_s = power supply output voltage in volts

The average power per pulse is given as

$$\overline{P_{pulse}} = \frac{1}{\tau} \int_0^{\tau} \frac{e^2(t)}{R_L} \, dt \tag{51}$$

where:

$\tau = 10^{-3}$ seconds

$e(t)$ = PFN output pulse voltage in volts

$R_L = 1.75$ ohms

The integration for Eq. 51 was carried out graphically as shown in Fig. 16. The resulting pulse power is

$$P_{pulse} = \frac{79.2}{17.5} = 4.53 \text{ kw} \tag{52}$$

The average power output is defined as

$$P_{out} = \frac{\text{pulse power}}{\text{pulse repetition rate}} = \frac{4.53 \times 10^3}{20} = 226 \text{ watts} \tag{53}$$

The resulting efficiency is

$$\eta = \frac{P_{out}}{P_{in}} = \frac{226}{285} = 0.794 \tag{54}$$

It is not sufficient to discuss efficiency just in terms of power transfer. In this case, it may be more meaningful to describe the requirements of the pulse generator in terms of energy transfer and output pulse shape. The pulse generator must deliver, to the klystron, 4.8 joules of energy in one millisecond. The pulse shown in Fig. 15 does not quite meet the energy output requirement. The energy output is only 4.53 joules instead of the required 4.8 joules.

The voltage level cannot be increased because this would adversely effect the klystron. Therefore, the only thing that can be done to increase the energy in the pulse is to increase its duration. This could be accomplished by increasing the capacitance values some small amount. One adverse effect of doing this is that it will reduce the PFN characteristic impedance causing a poorer match with the load (Re: Eq. 5). A final determination of element values can only be made with the pulse generator actually driving the klystron under operating conditions. In any case, the adjustments would be minor and we can assume that the power requirement can be met without too much difficulty.

E. ENVIRONMENTAL TESTING

In order to insure a degree of space flight worthiness, the PFN inductors and the charging reactor were tested in a hot-cold chamber. The inductors alone were tested because it was felt that they were the most critical items since they were all handmade. The capacitors that were used in the breadboard model would not be used in a final version of this PFN and there was no point in testing them.

The inductors were enclosed in the hot-cold chamber and the test pulse generator was operated with full operating voltage levels at -25°C for two hours and at +50°C for two additional hours. The output pulse waveform was monitored for this entire period and no change in shape or level was perceived.

CHAPTER IV

SUMMARY AND CONCLUSIONS

A. SUMMARY

This problem originated when the Electronic Systems Laboratory at M.I.T. constructed a breadboard model of a space vehicle radar system for making measurements of the reflectivity of the surface of Venus. This breadboard model had a line-type pulse generator which used a PFN that was 22 inches long and weighed about fifteen pounds. It was desired to minimize the size and weight of the entire pulse generator. The PFN was the largest and heaviest item and it was felt that if it could be optimized, then the entire pulse generator would also be optimized. Subsequent investigations verified this assumption.

The first step in the investigation of the problem was to make a study of the proposed line-type modulator to determine the parameters that described the optimum PFN and hence the optimum pulse generator. A guiding factor in the determination of the PFN was that the associated components, such as the pulse transformer and the charging reactor, had to be physically realizable. It was assumed that the study would reveal the combination of these components that resulted in the smallest and lightest weight complete pulse generator. This is what the study revealed, the details of which are in Appendix A, but there was the unexpected additional result that the physical size and weight of the pulse transformer was independent of other parameters for the three values of power supply voltage that were assumed.

The power supply that would be used in the complete system is capable of operation at any fixed level between 300 and 500 volts. For this reason, the values of power supply voltage taken for the study were

300, 400, and 500 volts. For each of these three operating values, the pulse transformer had a calculated weight figure of about 2.5 pounds. This is less than the complete transformer would actually weigh because the weight of insulation and packaging was not considered. This weight figure indicated that any of the supply voltage levels was satisfactory and that final determination rested on the value that optimized the PFN, which was the original assumption.

Two factors indicated that the lowest power supply level should be chosen. First, the higher voltage levels would require heavier insulation in the inductor coil construction, and second, the higher voltage levels would require more turns in each coil to prevent saturation. A final factor was the relative ease in obtaining 600 volt SCR's as compared to 1,000 volt SCR's for use as the switching devices.

There were two factors that made the design and construction of this PFN a difficult problem. These are the high power and long pulse duration. It was felt that the size and weight of the PFN could be reduced considerably by using ferrite core inductors. The inductors had to be made linear, however, to obtain a satisfactory output pulse waveform. This meant that the core material had to be one that had a linear permeability throughout its range of flux density. This led to the examination of the "square loop" materials and Z-type "Hypersil" was selected because it has a higher saturation flux density than the other materials considered. One small problem with this material was that it was readily available only in certain standard sizes.[8] The manufacturer's delivery time on these "stock" sizes was two-to-three weeks, and the non-standard items had to be specifically made and took up to nine weeks for delivery. For this reason

one of the more readily available H-type Hypersil cores was used in the construction and testing of the PFN.

The completed PFN inductors are shown in Fig. 11a with a reference scale to indicate their size. The important characteristics of these inductors is listed in Table 7. The statistics for the charging reactor that was used in the tests is also included in the table to indicate how it compares to the one used with the original PFN which weighed 5.8 pounds.

Table 7

Summary of PFN Inductor Characteristics

Inductor	Core	Wire Size (AWG)	Number of Turns	Resistance (ohms)	Total Weight (lbs)
L_1	Z-216	19	442	1.11	0.917
L_2	H-41	22	280	1.04	0.312
L_3	Z-1	24	230	1.10	0.187
L_4	Z-4	24	290	1.24	0.129
L_5	Z-2	24	253	1.22	0.099
		Total Weight of PFN Inductors			1.644 lbs
L_c	Z-5	22	500	3.84	0.790
		Total Weight of All Inductors			2.434 lbs

The small size and weight of the PFN inductors is significant. The capacitors used in the final version of this PFN weighed four pounds bringing the total PFN weight to 5.6 pounds. This weight can be reduced considerably by having capacitors specially manufactured to meet space application requirements. Consideration was given to the fact that the highest operating voltage

required the smallest amount of capacitance. Since these items contribute considerable weight to the PFN a superficial examination would indicate that the capacitors will be lighter if the PFN is designed to operate at the highest voltage. This is not true, however, because although less capacitance may be required, the units are larger and heavier than for a similar lower voltage rating and no net savings can be realized.

The original PFN, shown in Fig. 2, weighs fifteen pounds and is twenty-two inches long. This new PFN, shown in Fig. 11a, weighs only about one-third as much and could be packaged in about six inches by four inches by four inches depending upon the capacitors and the arrangement used.

The efficiency figure for the PFN, given in Chapter III as 79.4%, is reasonable considering that a certain amount of loss was designed into the PFN in order to make it compact. Some saving in power could be realized by reducing the resistance of the charging reactor by making the coil larger. Although this would certainly improve the efficiency figure given above it still may not be a desirable thing to do. Any increase in coil size would have to be accompanied by a larger core and the additional weight may be more undesirable. This efficiency figure also does not include any loss that would be incurred by resetting a pulse transformer by the method described in Appendix A.

In conclusion, the PFN that was constructed and tested provides a satisfactory answer to the problem of size and weight. It is reliable, efficient, and operates satisfactorily over a wide range of temperatures. It produces a pulse waveform that meets all the requirements but energy

content. This deficiency is small, however, and can be easily corrected by making the pulse duration a little longer by increasing the capacitance a small amount.

The circuit that was used to test the PFN is a complete pulse generator with the exceptions of a pulse transformer and proper power supply. It is also the optimum pulse generator of this type for this application. With refinements in the timing circuitry to meet environmental requirements it would be ready for further application in the complete radar system.

APPENDIX A

A PARAMETRIC STUDY OF THE OPTIMUM PULSE GENERATOR

The object of this thesis is an optimum PFN as described in Chapter II. The initial step in the construction of this PFN is to determine the supply voltage at which the system will be operated. The power supply voltage that would be used in the pulse generator can be any level from 300 to 500 volts. This appendix studies the effect of power supply voltage on the components of the pulse generator. All calculations are based upon three values of E_s as shown in Table 8.

A. THE PULSE TRANSFORMER

The elementary theory of pulse transformers[1] is sufficient for the purpose of describing the smallest possible transformer that will work in this pulse generator. The actual construction design of this transformer must consider details of minimum distortion of the pulse shape, efficiency, and ease of construction. These items will not be evaluated here since they are not too important in the determination of size and operating voltage.

A simplified model of a transformer is given in Fig. 18. The relationships between primary and secondary quantities are

$$I_p E_p = I_s E_s \tag{55}$$

$$I_p = N I_s \tag{56}$$

$$E_p = \frac{E_s}{N} \tag{57}$$

$$\frac{E_p}{I_p} = \frac{E_s / I_s}{N^2} \tag{58}$$

The transformer being considered here will drive a klystron with an input pulse of 4.8 kw at 8,000 volts.

$$E_s = E_o = 8,000 \text{ volts} \tag{59}$$

$$I_s = I_o = 0.60 \text{ amps.} \tag{60}$$

$$\frac{E_s}{I_s} = 13,300 \text{ ohms} \tag{61}$$

This pulse transformer must meet the following specifications: 1) must not saturate during a pulse, 2) must not store a large amount of residual magnetic energy during a pulse, 3) must have low resistive losses, and 4) must be compact and light weight.

If the voltage input to the primary is in the form of a rectangular pulse,

$$\int_0^T e(t)dt = ET \tag{62}$$

Because the transformer will be reset between pulses, a gapless toroidal core, as shown in Fig. 8b, can be used. This may complicate construction, but it does not make the transformer unfeasible. The core will not saturate during a pulse if the turns-cross section product satisfies

$$NA = \frac{ET}{\Delta B} \tag{63}$$

The number of turns in the primary winding must be sufficient to keep the residual magnetizing current to a minimum at the end of a pulse. A reasonable figure that gives good results is that magnetizing current should be less than five percent of load current.

$$I_m = 0.05 \times I_p \tag{64}$$

The primary inductance is given by

$$I_m L_p = \int_0^T e(t)\, dt \tag{65}$$

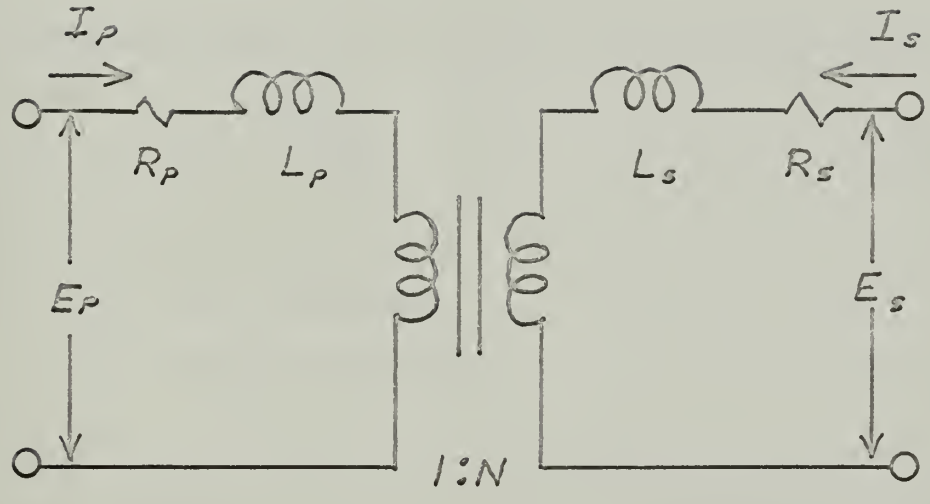

FIG. 18

SIMPLIFIED PULSE TRANSFORMER MODEL

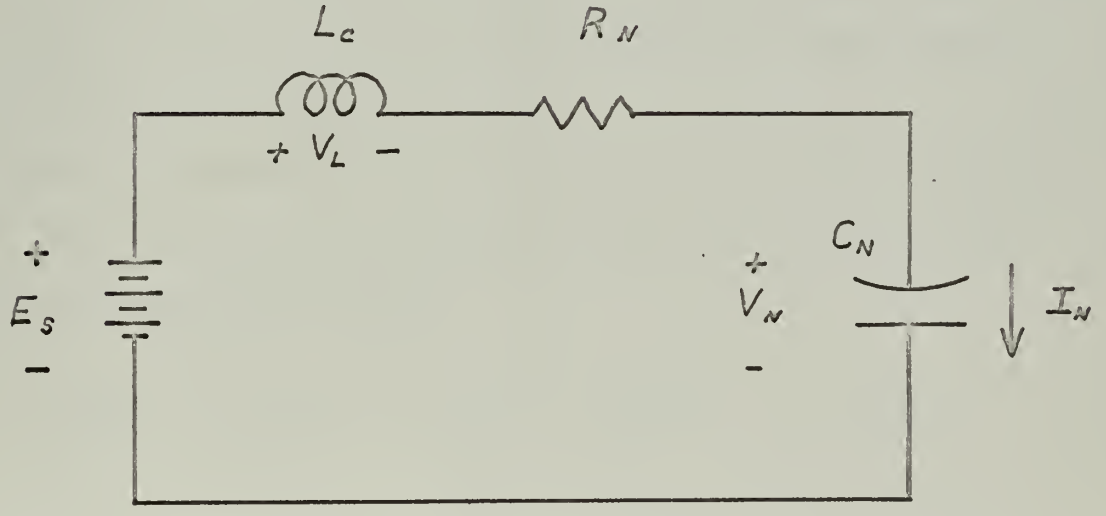

FIG. 19

EQUIVALENT CHARGING NETWORK

$$L_p = \frac{E_p T}{I_m} \tag{66}$$

In addition, the primary inductance is related to the core material by

$$L_p = \frac{N^2 A \mu_c}{l_m} \tag{67}$$

A = core cross section

μ_c = core permeability

l_m = magnetic path length

Z-type Hypersil has an incremental permeability of approximately 8,000 over the operating range of flux density.[8] This figure gives reasonable answers but is probably lower than the actual permeability. The value of permeability taken as the average slope of the d-c.B-H curve between operating limits is about 44,000.[7] This value is higher than can be expected because the frequency components of the pulse are at least 500 CPS. The lower of these two values of permeability is used for all calculations to allow for the higher frequency components.

Calculations were made for several toroidal cores before a choice was reached. However, only the calculations for the Z-361 core are shown since this is the one finally selected.

Core	Volume (in3)	A(in^2)	ℓ_m (in)	Window (in^2)	Weight (lbs)
Z-361	7.85	1.00	7.85	3.14	1.95

Assume source voltage of 300 volts.

Primary turns:

$$N_p = \frac{300 \times 10^{-3}}{(6.45 \times 10^{-4})(2.9)} = 160 \text{ turns} \tag{68}$$

Secondary turns:

$$\text{Turns ratio} = \frac{8,000}{300} = 26.7 \tag{69}$$

$$N_s = (26.7)(160) = 4,275 \text{ turns}$$

The winding resistance is determined by limiting it to five percent of the load impedance.

$$R_{primary} = (0.05)(18.7) = 0.97 \text{ ohms}$$

$$R_{secondary} = (0.05)(13,300) = 665 \text{ ohms}$$

The average length of a winding turn calculated from the core geometry is approximately

$$\ell_c = F + 2E + 2D = 0.583 \text{ feet} \tag{70}$$

Primary winding resistance

$$r_w = \frac{(1)(1,000)}{(160)(0.583)} = 10.5 \text{ ohms/1,000 ft.} \tag{71}$$

This corresponds to number 20 wire.

Secondary winding resistance

$$r_w = \frac{(665)(1,000)}{(4,275)(0.583)} = 266 \text{ ohms/1,000 ft.} \tag{72}$$

This corresponds to number 34 wire.

The winding stacking factor was determined by examining a pulse transformer in the laboratory. This transformer has a primary widning consisting of 400 turns of number 24 wire and a secondary winding consisting of 4,200 turns of number 32 wire. The primary and secondary voltages are 300 volts and 8,000 volts, respectively. The core window area is 2.06 square inches which is completely filled with wire and insulation. By taking the total wire area and dividing by the window area a stacking factor was determined for use in further calculations.

X = (Number primary turns)(Area of no. 20 wire)
+ (Number secondary turns)(Area of no. 32 wire) /window area (73)

X = Stacking factor = 0.163 turns

In addition, a hole large enough to pass a winding shuttle must be left in the center of the window. Most shuttles can be accommodated by a one-inch diameter hole. Therefore, an area of 0.785 square inches must be subtracted from the core window area.

The window area required to accommodate the windings can now be obtained from Eq. 73.

$$\text{Window area required} = \frac{(160)(0.000802) + (4.275)(0.000031)}{0.163}$$

$$= 1.6 \text{ square inches}$$

Available window area = 3.14 - 0.785 = 2.36 square inches

If the weight of insulating materials and other attachments such as terminals is ignored, a measure of the total transformer weight can be calculated for comparision purposes.

Weight of winding = (Number of turns)(Weight of wire)(ℓ_c) (74)

Primary winding = (160)(0.00309)(0.583) = 0.288 lbs.

Secondary winding = (4,275)(0.00012)(0.583) = 0.300 lbs.

Total coil weight = 0.588

Core weight = 1.950

Transformer weight = 2.538 (75)

Primary inductance is

$$L_p = \frac{(160)^2(6.45 \times 10^{-4})(8,000)(4\pi \times 10^{-7})}{0.20} = 0.832 \text{ henry} \quad (76)$$

The minimum primary inductance required is

$$L_p = \frac{300 \times 10^{-3}}{0.8} = 0.375 \text{ henry} \qquad (77)$$

These calculations show that the Z-361 core is adequate in all respects. Similar calculations for supply voltages of 400 volts and 500 volts show that the same core can be used.

The results shown in Table 8 are interesting because they show that pulse transformer size is independent of the supply voltage. This means that the size of the optimum pulse generator depends solely on the PFN and charging reactor. All other elements are fixed in size by the power handling requirements.

Table 8

Summary of Pulse Generator Parameters and Pulse Transformer Characteristics

Supply voltage	E_s	Volts	300.0	400.0	500.0
Char. impedance	Z_n	Ohms	18.7	33.3	52.0
Total PFN cap.	C_n	μf	26.7	15.0	9.6
Total PFN ind.	L_n	mh	9.35	16.7	26.0
Load current	I_o	Amps	0.6	0.6	0.6
Load voltage	E_o	Volts	8000.0	8000.0	8000.0
Primary current	I_p	Amps	16.0	12.0	9.6
Pri. mag. current	I_m	Amps	0.80	0.60	0.48
Trans. turns ratio	N	Turns	26.7	20.0	16.0
No. pri. turns	N_p	Turns	160.0	214.0	267.0
Pri. wire size		Number	20.0	21.0	22.0
No. sec. turns	N_s	Turns	4275.0	4275.0	4275.0
Sec. wire size		Number	34.0	34.0	34.0

Table 8 (Continued)

Max. pri. resistance	R_p	Ohms	1.0	1.67	2.60
Max. sec. resistance	R_s	Ohms	665.0	665.0	665.0
Min. pri. induct.	L_p	Henry	0.3	0.667	1.04
Calc. pri. induct.	L_p	Henry	0.832	1.49	2.32
Pri. coil weight		lbs.	0.288	0.305	0.340
Sec. coil weight		lbs.	0.300	0.300	0.300
Core weight		lbs.	1.950	1.950	1.950
Total weight		lbs.	2.538	2.555	2.590

B. THE CHARGING REACTOR

The principle of resonant charging[5] is used to charge the PFN to approximately twice the supply voltage. This method works best when the resistive losses in the charging network are small and the value of charging inductance is large with respect to the total inductance of the PFN. If these conditions are met, the equivalent charging circuit is shown in Fig. 19. Solution of this network, with assumed zero initial conditions, is[1]

$$v_n(t) = E_s\left[1 - e^{-\alpha t}\left(\cos \omega t + \frac{a}{\omega} \sin \omega t\right)\right] \tag{78}$$

$$i_n(t) = \frac{E_s}{\omega L_c} e^{-\alpha t} \sin \omega t \tag{79}$$

where:

$$\alpha = \frac{R}{2L_c} \tag{80}$$

R = total network resistance

L_c = inductance of charging reactor

$$\omega = \left(\frac{1}{L_c C_n} - \frac{R^2}{4L_c^2}\right)^{1/2} \tag{81}$$

C_n = total PFN capacitance

If losses are small, the solutions reduce to the approximations

$$v_n(t) = E_s(1-\cos \omega t) \tag{82}$$

$$i_n(t) = \frac{E_s}{\omega L_c} \sin \omega t \tag{83}$$

The PFN voltage will reach a maximum of $2E_s$ when $t = \pi\sqrt{L_c C_n}$. At this time network current will be zero.

The normal method of applying this principle is to trigger the PFN discharge at the resonant frequency ω, in which case the PFN is discharged completely and then allowed to charge again with the repetition rate

$$T_r = \pi\sqrt{L_c C_n} \tag{84}$$

It is not disirable to do this here because it would require a very large charging reactor. Figure 2 shows the charging reactor that was required with the original PFN by using this principle. The use of a charging SCR allows the charging inductance to be made as small as desired. In this case the practical lower limit on L_c is about ten times L_n. Any value smaller than this will not justify ignoring L_n in the calculations. A value much larger will cause two complications. First, the charging period will become excessively long. Secondly, an SCR generally requires about 30 to 150 ma of gate current, sustained for several microseconds, to turn it on;[9] if the reactance of L_c is too large, the SCR will not fire because the timing pulses are only about ten microseconds long. A value of L_c = 130 mh was found to be satisfactory. The calculations for this reactor using a Z-5 core are similar to those for L_1 given previously. The value of v(t) from Eq. 86 must be used in place of e(t) in Eq. 13.

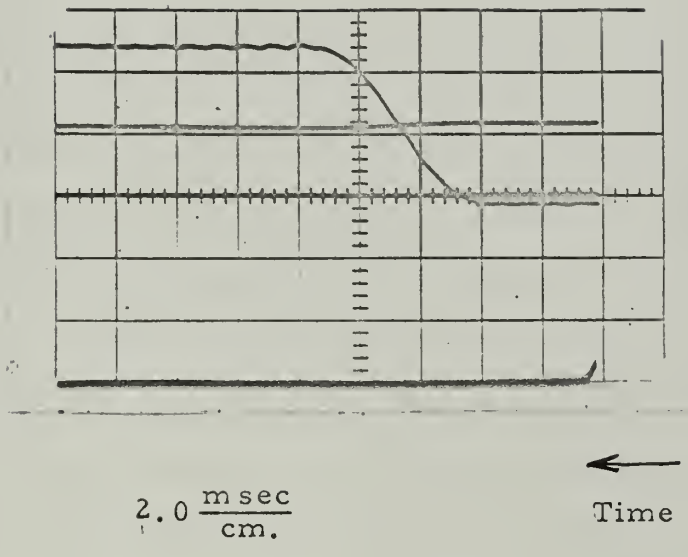

Fig. 20 Power Supply Level and DC Resonant Charging of PFN

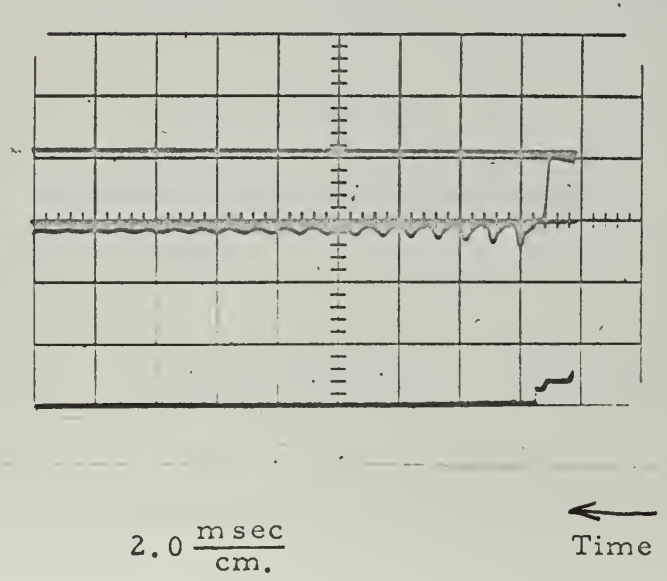

Fig. 21 PFN Oscillations After an Output Pulse

The charging period is

$$T_c = (130 \times 10^{-3} \times 19.7 \times 10^{-6})^{\frac{1}{2}} = 5.05 \text{ ms} \quad (85)$$

Figure 20 shows the PFN voltage and power supply voltage during the charging period. The small ripples on the PFN voltage in Fig. 20 are shown more clearly in Fig. 21. In this figure, the PFN is not allowed to recharge at the end of a pulse and the ripples show up as a damped oscillation. This is the result of the PFN not being perfectly matched to the load. The slight mismatch is shown in Fig. 15 as a small reflection of the load pulse. This mismatch is required to insure that the discharge SCR is turned off at the end of a pulse. The PFN voltage is not zero at the end of a pulse when the SCR stops conducting, the PFN losses are very small and it therefore oscillates with little damping. These oscillations in no way adversely effect the pulse generator operation since they do not appear across the load.

The possibility of eliminating the charging reactor completely by using the primary winding of the pulse transformer in its place has been considered. The voltage across a reactor L, as in Fig. 19, is

$$v_L(t) = E_s \cos \omega t \quad (86)$$

The reactor must not saturate during the charging interval. This corresponds to satisfying the equation

$$\Delta B \, NA = \int_0^{T_c} v(t)dt = E_s \sqrt{L C_n} \sin (\pi L C_n) \quad (87)$$

If L is taken as the calculated transformer primary winding inductance from Table 8, this reduces to

$$\Delta B \, NA = (E_s)(208 \times 10^{-9}) \quad (88)$$

whereas the pulse transformer was designed to satisfy

$$\Delta B \, NA = E_s \times 10^{-3} \quad (89)$$

The difference between Eq. 88 and Eq. 89 indicates that the pulse transformer would not be reset in the charging process and that it would most likely saturate during the next pulse. There are three solutions to this: 1) use a cut-core with an air gap, which would result in a much larger transformer, 2) reset the gapless core from an external source, or 3) use a separate charging reactor. The third solution is the most acceptable since it will lead to the lightest pulse generator. But, the pulse transformer must be reset during the charging period. This requires that a large voltage appear across the transformer primary winding in order to reverse saturate the core.

In order to protect the klystron from large negative fly-back voltages, the series combination of D_k and R_k is used. The diode protects the klystron while the resistor provides the necessary voltage to reset the pulse transformer. The equivalent charging circuit becomes similar to that of Fig. 19. The assumptions are that the primary winding reactance is much larger than R_k and that R_k is much larger than R_n. The voltage across R_k is approximately

$$v_{R_k}(t) = R_k \frac{E_s}{L_c} \sin \omega t \tag{90}$$

Substituting

$$\omega = \frac{1}{\sqrt{L_c C_n}} \tag{91}$$

yields

$$v_{R_k}(t)dt = \frac{2R_k E_s}{\omega^2 L_c} = 2R_k E_s C_n \tag{92}$$

Therefore, the value of R_k required to reset the pulse transformer during the charging period is

$$R_k = \frac{N^2 \times 10^{-3}}{2C_n} = \frac{(26.7)^2 \times 10^{-3}}{39.4 \times 10^{-6}} = 18,000 \text{ ohms} \qquad (93)$$

The charging efficiency of the system will be reduced due to damping by the resistances R_n and R_k. Instead of the PFN charging to approximately $2 \times E_s$, the final value, found from Eq. 78, will be about $1.6 \times E_s$. This corresponds to a required supply voltage of 375 volts in order to charge the PFN to 600 volts.

APPENDIX B

SILICON-CONTROLLED-RECTIFIER SWITCHING DEVICES AND TIMING CIRCUIT

When this thesis was first proposed, one of the questions that had to be investigated was whether or not SCR's could effectively be used as switching devices. At the time, commerically available SCR's had a maximum peak-forward-voltage rating of 850 volts.[9] There was, however, at least one manufacturer who indicated that an SCR with ratings of 1,200 volts and 110 amperes was available.[13] There was no indication of the availability and cost of this higher rated unit nor of its performance. This was a contributing factor when the power supply voltage was selected.

Once the power supply voltage had been determined as 300 volts, the SCR's were selected from the laboratory stock. A 2N-691 was used for SCR-1 and an unmarked SCR that was tested and found to have the proper voltage rating was used as SCR-2.

The characteristics of an SCR are given in detail in reference 9. The primary problems faced here were simply how to switch the SCR off and on at the proper times. The switching from conducting to non-conducting states can be accomplished by two means; 1) interrupt the flow of current by opening the circuit or 2) apply a negative voltage from anode to cathode. The first method is used to turn off SCR-1. When the PFN voltage reaches a maximum during charging, the charging current, through SCR-1, is zero and the SCR stops conducting until triggered again. The second method is used for SCR-2. The mismatch between the load and PFN characteristic impedance causes a small negative step at the end of the pulse which is sufficient to cause SCR-2 to stop conducting.

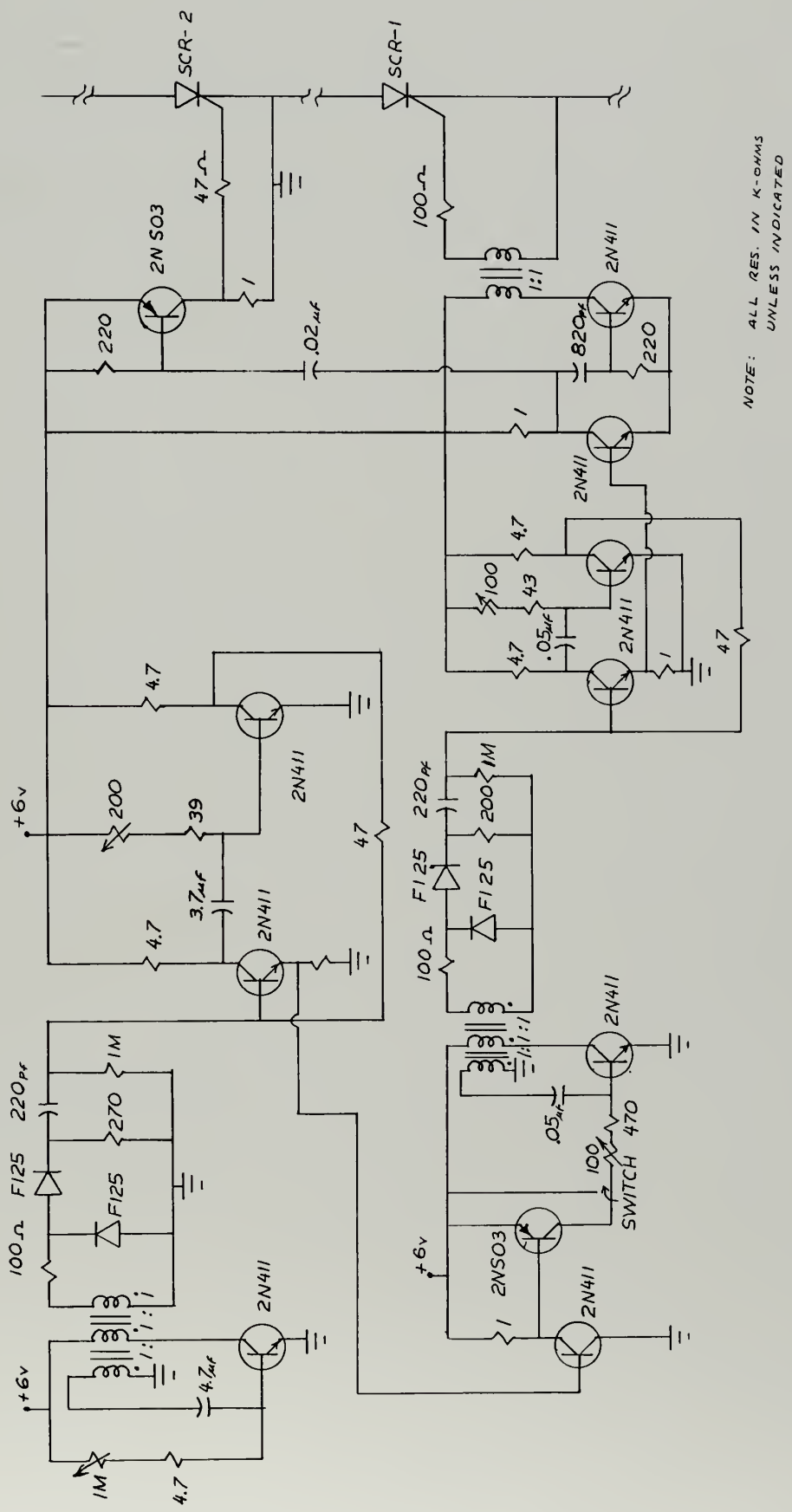

FIG. 22 PULSE GENERATOR TIMING CIRCUIT

In order to trigger the SCR's on at the proper times, the circuit of Fig. 22 was constructed. Basically, this circuit produces two sets of timing pulses as shown in Fig. 23. In each set, the pulses are twenty milliseconds apart and the two sets of pulses can be shifted with respect to one another. One set of pulses is used to trigger SCR-1 for charging the PFN and the other set is used to trigger SCR-2 to discharge the PFN. The amount of the offset between the sets of pulses merely determines the delay between charging the PFN and discharging it.

The timing circuit is capable of operating continuously at a pulse repetition rate between five and twenty-five milliseconds or, by closing the toggle switch, as a burst generator that will produce a four pulse burst at intervals from one-half second to about five seconds. The burst-repetition rate was decreased from the required fifteen second interval, as shown in Fig. 1, to more easily view the tests by oscilloscope.

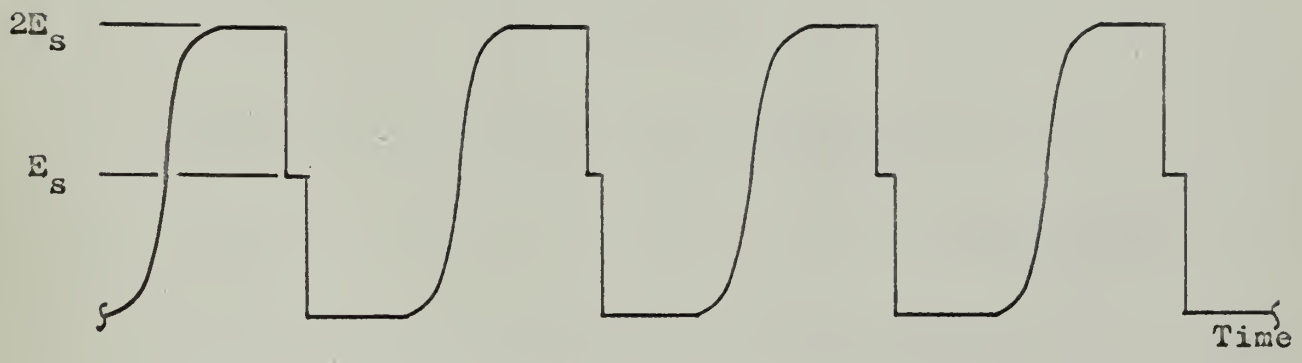

PFN VOLTAGE

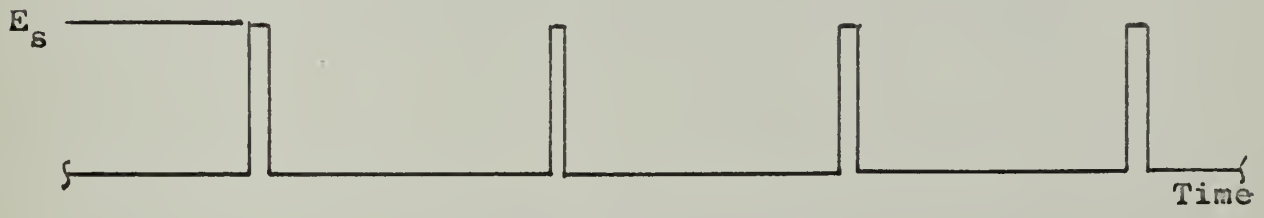

PFN OUTPUT PULSES

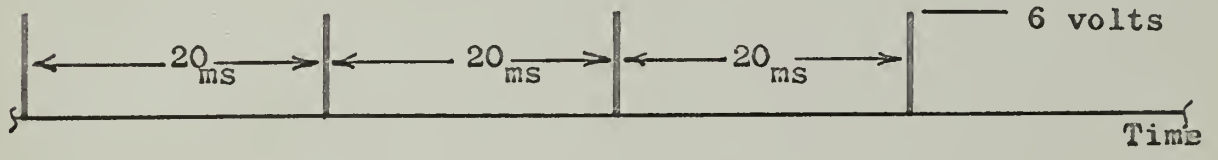

TIMING CIRCUIT CHARGING PULSES

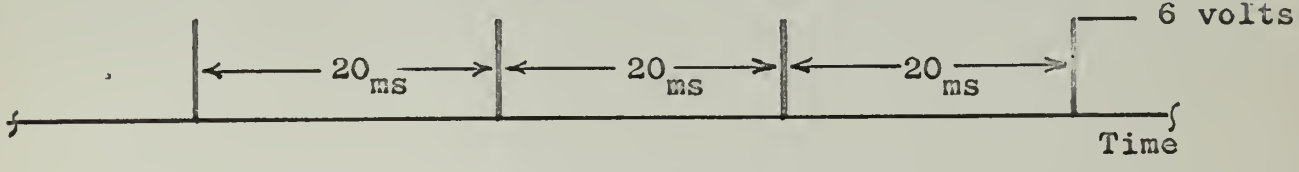

TIMING CIRCUIT DISCHARGING PULSES

FIG. 23 TIMING PULSES

BIBLIOGRAPHY

1. Glasoe, G.N. and Lebacqz, J.V.; "Pulse Generators", Radiation Laboratory Series; McGraw-Hill, 1948..

2. Weiss, H.G., "Haystack Microwave Facility", IEEE Spectrum, February, 1965.

3. Roberge, J.K., "Design of Spacecraft Radar Systems for Investigation of the Planet Venus", Electronic Systems Laboratory, M.I.T., 1962.

4. Dertouzos, M.L. and Bosco, J.A., "Design of a Radar System for Measuring the Electromagnetic Reflection Characteristics of the Earth's Surface from a Satellite", Electronic Systems Laboratory, M.I.T., 9461-M5, September, 1963.

5. Reintjes, J.F. and Coate, G.T., "Principles of Radar", McGraw-Hill, 1950.

6. Jordan, R.L., "Semi-Conductor Magnetic Pulse Generators", S.M. Thesis, M.I.T., 1962.

7. Arnold Engineering Company Bulletin SC - 107A, March, 1963.

8. Westinghouse Company Descriptive Bulletin 44 - 550, December, 1960.

9. General Electric Company, "Silicon-Controlled Rectifier Manual", 1961.

10. M.I.T. Department of Electrical Engineering Notes for Experimental Electronics Laboratory, 1963.

11. Terman, F.E., "Radio Engineers Handbook", McGraw-Hill, 1943.

12. International Telephone and Telegraph Corporation, "Reference Data for Engineers", American Book - Stratford Press, 1956.

13. Texas Instrument Newsletter, Volume 2, Issue 3, October, 1964.